

The Islamic University of Gaza
Deanery of Graduate Studies
Faculty of Engineering
Electrical Engineering Department



RE-EVALUATION AND RE-DESIGN STAND-ALONE PV SOLAR LIGHTING PROJECTS IN GAZA STRIP, PALESTINE

By

Shadi N. AlBarqouni

Supervisor

Dr. Mohammed T. Hussein

“A Thesis Submitted in Partial Fulfillment of the Requirements for
the Degree of Master of Science in Electrical Engineering”

The Islamic University of Gaza, Palestine

1431ھ – 2010م


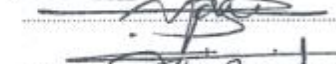



نتيجة الحكم على أطروحة ماجستير

بناءً على موافقة عمادة الدراسات العليا بالجامعة الإسلامية بغزة على تشكيل لجنة الحكم على أطروحة الباحث/ شادي نبيل محي الدين البرقوني لتبيل درجة الماجستير في كلية الهندسة قسم الهندسة الكهربائية/أنظمة التحكم وموضوعها:

RE-EVALUATION AND RE-DESIGN STAND-ALONE PV SOLAR LIGHTING PROJECTS IN GAZA STRIP, PALESTINE

وبعد المناقشة العلنية التي تمت اليوم الأحد 18 جمادى الأولى 1431هـ، الموافق 2010/05/02 الساعة العاشرة صباحاً، اجتمعت لجنة الحكم على الأطروحة والمكونة من:

	مشرفاً ورئيساً	د. محمد توفيق حسين
	مناقشاً داخلياً	أ.د. محمد محمد عبد العاطي
	مناقشاً داخلياً	د. أنور محمد أبو ظريفة

وبعد المداولة أوصت اللجنة بمنح الباحث درجة الماجستير في كلية الهندسة / قسم الهندسة الكهربائية/أنظمة التحكم.

واللجنة إذ تمنحه هذه الدرجة فإنها توصيه بتقوى الله ولزوم طاعته وأن يسخر علمه في خدمة دينه ووطنه.

والله ولي التوفيق،،،

عميد الدراسات العليا



د. زياد إبراهيم مقداد

Abstract

Recently, with the critical situation of siege on Gaza Strip, the need of an alternative energy source instead of traditional energy sources becomes an urgent need, especially Palestine is considered one of the sunny countries and perceps good solar radiation over the year. In this research; the re-evaluation and re-design of a reliable control system process were analyzed step by step, beginning with modeling the global solar radiation passing through orientation and tilting, ending to PV and Battery sizing.

This thesis evaluates the previous lighting project implemented in Gaza Strip, and focuses on the critical drawbacks which are not considered in the existence design. The research results were tested by the utilization and implementation of an experimental solar model for lighting an apartment to validate the proposed solar control system taking into account the IEEE Recommendations.

Recommendations for Building Integrated Photovoltaic (BIPV) Designers and consultants are mentioned here to be considered for next solar projects and related studies.

ملخص البحث

مع الوضع الحرج والحصار المفروض على قطاع غزة منذ ما يقارب الأربعة أعوام ظهرت الحاجة إلى مصدر بديل للطاقة بدلاً من الطاقة التقليدية، وأصبح هذا الأمر ملحاً وخصوصاً مع استمرار انقطاع الطاقة الكهربائية وكذلك المحروقات عن قطاع غزة.

حيث تهدف هذه الدراسة البحثية إلى إعادة تقييم وتصميم أنظمة تحكم هندسية لمشاريع الإنارة التي تم تطبيقها في قطاع غزة في الآونة الأخيرة وتحليلها بدءاً من نمذجة الإشعاع الشمسي في فلسطين مروراً بأهمية التوجيه والإمالة للخلية الشمسية وانتهاءً بتصميم البطاريات والخلايا الشمسية، حيث تم التركيز على السليبيات الحاسمة للتصاميم السابقة وكيفية التغلب عليها.

لهذا الغرض أعد الباحث تجربة عملية (كنموذج تحكم هندسي) لإضاءة شقة من خلال الخلايا الشمسية مع أخذ بعين الاعتبار المعايير والتوصيات المقترحة من قبل جمعية مهندسي الكهرباء والالكترونيات العالمية (IEEE).

حيث خلص الباحث من خلال هذه الدراسة بوضع نتائج ودراسات منهجية على أسس علمية للاستفادة منها عند تصميم مشاريع مستقبلية.

ويوصي الباحث الاستشاريون والقائمون على غرار هذه المشاريع بالاستفادة من توصياته في هذا المجال للأخذ بها في عين الاعتبار في حال التصميم لمشاريع أنظمة تحكم في الطاقة الشمسية مستقبلاً.

Dedication

*To my parents, my darling who have been
a constant source of motivation, inspiration and support.*

Acknowledgments

I would like express my thanks to many people who have contributed to the success of this research, in particular my thesis supervisor Dr. Mohammed T. Hussein, for his support, encouragement, and continuous follow-up of this research.

I would like also to extend my gratitude and appreciation to thesis committee, both Prof. Dr. Mohammed Abdelati and Dr. Anwar Abu Zarifa for their suggestions and recommendations that helped with the development of this research, greeting to Dr. Mahir Sabra for his support.

Special thanks to the Engineers and Consultants in Authority of Energy, who helped me in this research, also special thanks to El-Wafa Charitable Society in Gaza City for their partial financial support to this project.

Special greetings to my family, especially my parents, who have always kept me in their prayers, who have suffered a lot to make me happy.

Contents

Abstract	iii
Dedication	v
Acknowledgments	vi
List of Tables	x
List of Figures	xi
1 Introduction and Literature Review	1
1.1 Introduction to Renewable Energy	1
1.1.1 Biomass Energy	1
1.1.2 Wind Energy	3
1.1.3 Geothermal Energy	4
1.1.4 Photovoltaic Solar Energy	5
1.2 Research Motivation and Goal	7
1.2.1 PV Modules	8
1.2.2 Controllers	8
1.2.3 Batteries	8
1.2.4 Safety and Maintenance	8
1.2.5 Cost vs. Quality	8
1.3 Literature Review	10
1.3.1 Modeling of Global Radiation Model	10
1.3.2 Orientation and Tilt Angles	10
1.3.3 PV system Model	11
1.3.4 PV Modules, Batteries, MPPT Controllers and Regulators	11
1.3.5 Maintenance and Monitoring	12
1.4 Research Results and Contributions	12
1.5 Thesis Structure	13
2 Developing Empirical Models for Estimating Global Solar Radiation	14
2.1 Introduction	14

2.2	Background	14
2.3	Methodology	15
2.3.1	Data	15
2.3.2	Description of the Model	16
2.3.3	MATLAB Program	18
2.4	Results and Discussion	18
2.5	Conclusion	22
3	Optimum Tilt Angle & Orientation for PV Panels	23
3.1	Introduction	23
3.2	Earth – Sun Geometry	23
3.3	Methodology and Design	25
3.3.1	Definition of Angles	25
3.3.2	Derivation of Solar Angle $\cos\theta_s$ ($\sin\alpha_s$):	27
3.3.3	Derivation the Optimum Tilt and Azimuth angles for the Solar Plate	29
3.3.4	Computing the Solar Angle $\cos\theta_s$	30
3.3.5	Enhancement on the Optimum Values	31
3.4	Implementation	33
3.5	Discussion and Conclusion	36
4	PV System Components: PV Modules, Batteries & Charge Controllers	38
4.1	Introduction	38
4.2	PV Modules	38
4.2.1	Crystalline silicon PV modules	38
4.2.2	Amorphous silicon (a-Si) PV modules	40
4.2.3	Copper indium diselenide (CIS) PV modules	40
4.2.4	Cadmium telluride (CdTe) PV modules	41
4.2.5	Heterojunction with intrinsic thin layer (HIT) PV modules	41
4.3	Batteries	42
4.3.1	Capacity	42

4.3.2	Type	42
4.3.3	Cyclability	43
4.4	Charge Controllers	44
4.4.1	Shunt Regulator	44
4.4.2	Series Regulator	44
4.4.3	PWM Regulators	45
4.4.4	MPPT Controllers	46
4.5	PV & Battery Sizing	47
4.6	Discussion and Conclusion	50
5	Experimental Model: Stand-Alone Photovoltaic System for Home Lighting	51
5.1	Introduction	51
5.2	System Design & Implementation	52
5.2.1	Orientation and Tilt angle	52
5.2.2	Calculating Load Consumption	52
5.2.3	PV Components	53
5.3	Results and Discussion	56
5.3.1	PV and Battery Sizing	56
5.3.2	Cost Estimation	57
5.3.3	Conclusion	58
6	Conclusions and Recommendations	59
6.1	Introduction	59
6.2	Conclusion	59
6.3	Recommendation and Future Works	60
	References	61
	Appendices	65
A	Technical Specification	65
B	MATLAB Code	68
C	Abbreviation	72

List of Tables

Table 2.1: Location of stations and period of observation of global solar radiation	15
Table 2.2: Input Parameters for Angstrom's Equations	19
Table 2.3: Comparison between the observed and estimated global solar radiation for Gaza Strip	20
Table 2.4: Deviations between the estimated model and the observed global solar radiation data	21
Table 3.1: Mean values of solar angles for different tilt and azimuth angles	31
Table 3.2: Comparison between current and optimum orientation	34
Table 3.3: Comparison between various orientations	36
Table 4.1: Difference of Sizing Summery between current and recommended designs with same and different selected batteries and modules	50
Table 5.1 : Apartment Electrical Load	53
Table 5.2: Sizing Summery for an Apartment	57
Table 5.3: Sizing Summery for proposed model	57
Table 5.4: Comparison for cost estimation between available source energy for home user	58

List of Figures

Figure 1.1: Biomass Energy Cycle	2
Figure 1.2: offshore wind turbines	4
Figure 1.3: Geothermal energy process	5
Figure 1.4: Yearly som of direct beam insolation in the world	6
Figure 1.5: Solar Street lighting of Jib Aldeeb Village in West Bank, Palestine	7
Figure 1.6: Re-Evaluation and Re-Design Process	2
Figure 1.7: Typical PV System	2
Figure 2.1: Location of Stations that record Global Solar Radiation	16
Figure 2.2: Earth-Sun Angles; Latitude, Declination Angle and Hour Angle	17
Figure 2.3: The Clearness Index for Gaza Strip, Palestine	19
Figure 2.4: Comparison between the estimated and the observed values	21
Figure 3.1: Earth revolution around sun	24
Figure 3.2: Sun path at Gaza along the year	25
Figure 3.3: Variation of Hour Angle	26
Figure 3.4: Variation of Declination Angle	26
Figure 3.5: Earth Surface coordinate system for Observer	27
Figure 3.6: Earth Surface coordinate system for tilted Observer	28
Figure 3.7: The Optimum Tilt Angle along the year	30
Figure 3.8: Values of Solar Angles in Degree for Optimum Tilt & Azimuth Angles	31
Figure 3.9: Empirical Models developed by Al Barqouni and Hussein	32
Figure 3.10: PV Panels supported with adjustable gear	33
Figure 3.11: Fixed Solar Panels for Lighting Gaza Valley way	33
Figure 3.12: Gaza Valley Way Map by Google Earth®	34
Figure 3.13: Current Orientation Vs. Optimum Orientation	35
Figure 3.14: Enhanced Orientation Vs. Optimum Orientation	35
Figure 3.15: Improvement in Solar Power Insolation	36
Figure 4.1: Solar Cells and Panels	39
Figure 4.2: Crystalline silicon PV modules	39
Figure 4.3: Amorphous silicon (a-Si) PV modules	40
Figure 4.4: Copper indium diselenide (CIS) PV modules	41
Figure 4.5: Vented Batteries	42
Figure 4.6: Valve-Regulated Batteries	43
Figure 4.7: Shunt Regulator	44

Figure 4.8: Series Regulator	45
Figure 4.9: PWM Regulator	46
Figure 4.10: MPPT Controllers	46
Figure 4.11: PV and Battery sizing software flowchart	48
Figure 4.12: PV and Battery sizing software interface	49
Figure 5.1: Schematic Diagram of Experimental Solar Model	51
Figure 5.2: Elevation View of Home from Google Earth®	52
Figure 5.3: Mounted PV Module on roof building	54
Figure 5.4: ENS1210 Solar charge Controller	55
Figure 5.5: ENS1210 Solar charge controller with changeover switch	55
Figure 5.6: 500W Inverter with changeover switch between grid network and solar system	56

Chapter 1

Introduction and Literature Review

1.1 Introduction to Renewable Energy

Renewable energy sources have been important for humans since the beginning of civilization. For centuries and in many ways, biomass has been used for heating, cooking, steam rising, and power generation, hydropower and wind energy, for movement and later for electricity production. Renewable energy sources generally depend on energy flows through the Earth's ecosystem from the insolation of the sun and the geothermal energy of the Earth.

Furthermore, many renewable technologies are suited to small off-grid applications, good for rural, remote areas, where energy is often crucial in human development. At the same time, such small energy systems can contribute to the local economy and create local jobs.

The natural energy flows through the Earth's ecosystem are immense, and the theoretical potential of what they can produce for human needs exceeds current energy consumption by many times. For example, solar power plants on one percent of the world's desert area would generate the world's entire electricity demand today. [1]

1.1.1 Biomass Energy

Biomass is a rather simple term for all organic material that stems from plants, trees, and crops. Biomass sources are therefore diverse, including organic waste streams, agricultural and forestry residues, as well as crops grown to produce heat, fuels, and electricity.

Dominating the traditional use of biomass, particularly in developing countries, is firewood for cooking and heating. Some traditional use is not sustainable because it may deprive local soils of needed nutrients, cause indoor and outdoor air pollution, and result in poor health.

Since the early 1990s biomass has gained considerable interest world-wide. It is carbon neutral when produced sustainably. Its geographic distribution is relatively even. It has the potential to produce modern energy carriers that are clean and convenient to use. It can make a large contribution to rural development. And its attractive costs make it a promising

energy source in many regions. With various technologies available to convert biomass into modern energy carriers, the application of commercial and modern biomass energy systems is growing in many countries.

The resource potential of biomass energy is much larger than current world energy consumption. But given the low conversion efficiency of solar to biomass energy (less than 1 percent), large areas are needed to produce modern energy carriers in substantial amounts. With agriculture modernized up to reasonable standards in various regions, and given the need to preserve and improve the world's natural areas, 700-1,400 million hectares may be available for biomass energy production well into the 21st century. This includes degraded, unproductive lands and excess agricultural lands. The availability of land for energy plantations strongly depends on the food supplies needed and on the possibilities for intensifying agricultural production in a sustainable way as the biomass energy cycle shown in Figure 1.1.



Figure 1.1: Biomass Energy Cycle

Biogas production is still under investigation and few demonstration projects are existing in Palestine. The Biogas potential in Palestine is over than 33 million m³. Biomass (wood and agricultural waste) is traditionally used for cooking and heating in rural areas. Being Palestine one of the many olive oil producing countries in the region, the interest now is directed to utilize the olive mill solid waste (OMSW) to be used as clean source of energy. The olive harvest season is all year round and so the OMSW as a raw material is also constantly available. The annual average amount of OMSW is around 76,000 tons. The

municipal solid waste in Palestine could be used as a source of energy, a new developing proposal projects were released by PEC to generate electricity from burning the wastes (WTE). The proposal project is for constructing an 18 MW waste to energy (WTE) power plant in order to get rid of municipal solid waste (MSW) of the northern provinces of the west bank; this is done by a controlled combustion of the wastes which is exploited generate electricity. Thus, converting MSW to a valuable material rather than being an environmental and economical burden [2].

1.1.2 Wind Energy

Wind energy, in common with other renewable energy sources, is broadly available but diffuse. Wind energy was widely used as a source of power before the industrial revolution, but later displaced by fossil fuel use because of differences in costs and reliability. The oil crises of the 1970s, however, triggered renewed interest in wind energy technology for grid-connected electricity production, water pumping, and power supply in remote areas. In recent decades enormous progress has been made in the development of wind turbines for electricity production. Around 1980 the first modern grid-connected wind turbines were installed. In 1990 about 2,000 megawatts of grid-connected wind power was in operation world-wide at the beginning of 2000, about 13,500 megawatts. In addition, more than 1 million water-pumping wind turbines (wind pumps), manufactured in many developing countries, supply water for livestock, mainly in remote areas. And tens of thousands of small battery-charging wind generators are operated in China, Mongolia, and Central Asia.

Because of the sensitivity to wind speed and altitude, determining the potential of wind energy at a specific site is not straightforward. More accurate meteorological measurements and wind energy maps and handbooks are being produced and mostly published, enabling wind project developers to better assess the long-term economic performance of their projects.

In densely populated countries the best sites on land are occupied, and public resistance makes it difficult to realize new projects at acceptable cost. That is why Denmark and the Netherlands are developing offshore projects as shown in Figure 1.2, despite less favorable economics. Sweden and the United Kingdom are developing offshore projects to preserve the landscape.

Based on available data and topographical features of Palestine, potential of wind energy seems to be limited to the mountains (elevation of about 1000m); regions of Nablus, Ramallah and Hebron where the speed surpass 5 m/s and the potential about 600 kwh/m². Initial studies shows that the wind regime is suitable for operating a wind turbine for wind power generation in city of Hebron in West Bank. Al-Ahli Hospital is located in the south-western part of Hebron at 1000m above sea level on a site of 27500 m². The average wind speed at 10 m could be as high as 6.2m/s in this region according to detailed data supplied by the Weather Authority [2].

The proposed and the required wind turbine(s) to be installed at Al-Ahli Hospital is expected to be around ~700KW total power production capacity, the following is the general outline of the tentative specifications for the required wind turbine [2].

- Annual Wind Average 7-10 m/s
- Max Cut-in Wind Speed 3 - 4 m/s
- Cut-out Wind Speed for excessive wind ≈ 25 m/s
- Hub Height 45 m- 55 m
- Nominal Power 750 kW
- Operating Atmospheric Temperature From -10° to 40°C
- Lower Tower Diameter 2-5 m
- Upper Tower Diameter 1.5-2 m

Wind atlas is in the developing process for Palestinian Territories. Further researches and more field measurements for wind are required. Utilization of wind could be feasible in some locations for cut-off electricity production and water pumping [2].



Figure 1.2: offshore wind turbines

1.1.3 Geothermal Energy

Geothermal energy has been used for bathing and washing for thousands of years, but it is only in the 20th century that it has been harnessed on a large scale for space heating, industrial energy use, and electricity production. Prince Piero Ginori Conti initiated electric power generation with geothermal steam at Larderello in Italy in 1904. The first large municipal district heating service started in Iceland in the 1930s.

Geothermal energy process that has been declared as shown in Figure 1.3 has been used commercially for some 70 years, and on the scale of hundreds of megawatts, 40 years, both for electricity generation and direct use. Its use has increased rapidly in the past three decades at about 9 percent a year in 1975-95 for electricity and at about 6 percent a year for direct use. Geothermal resources have been identified in more than 80 countries, with quantified records of geothermal use in 46.

The utilization of geothermal technology as a source of energy for heating and cooling has been started in Palestine during the MED-ENEC project in one of the ITEHAD subdivision villas in Ramallah city and through establishing the first company in the region utilize the geothermal energy in residential and commercial sectors called MENA Geothermal.

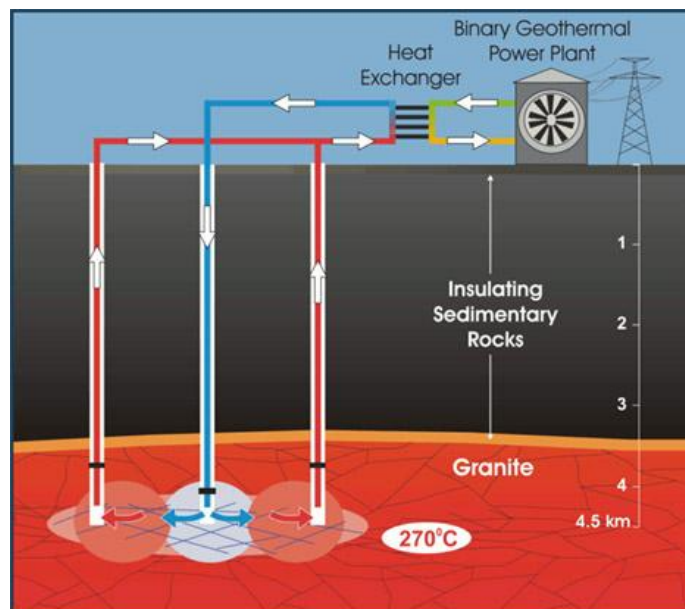


Figure 1.3: Geothermal energy process

1.1.4 Photovoltaic Solar Energy

Photovoltaic solar energy conversion is the direct conversion of sunlight into electricity. This can be done by flat plate and concentrator systems. An essential component of these systems is the solar cell, in which the photovoltaic effect the generation of free electrons using the energy of light particles takes place. These electrons are used to generate electricity.

Solar radiation is available at any location on the surface of the Earth. The maximum irradiance of sunlight on Earth is about 1,000 watts a square meter, irrespective of location. It is common to describe the solar source in terms of insolation the energy available per unit of area and per unit of time (such as kilo-watt-hours per square meter a year). Measured in a horizontal plane, annual insolation varies over the Earth's surface by a factor

of 3 from roughly 800 kilowatt-hours per square meter a year in northern Scandinavia and Canada to a maximum of 2,500 kilowatt-hours per square meter a year in some dry desert areas. The differences in average monthly insolation (June to December) can vary from 25 percent close to the equator to a factor of 10 in very northern and southern areas as shown in Figure 1.4, determining the annual production pattern of solar energy systems. The ratio of diffuse to total annual insolation can range from 10 percent for bright sunny areas to 60 percent or more for areas with a moderate climate, such as Western Europe. The actual ratio largely determines the type of solar energy technology that can be used.

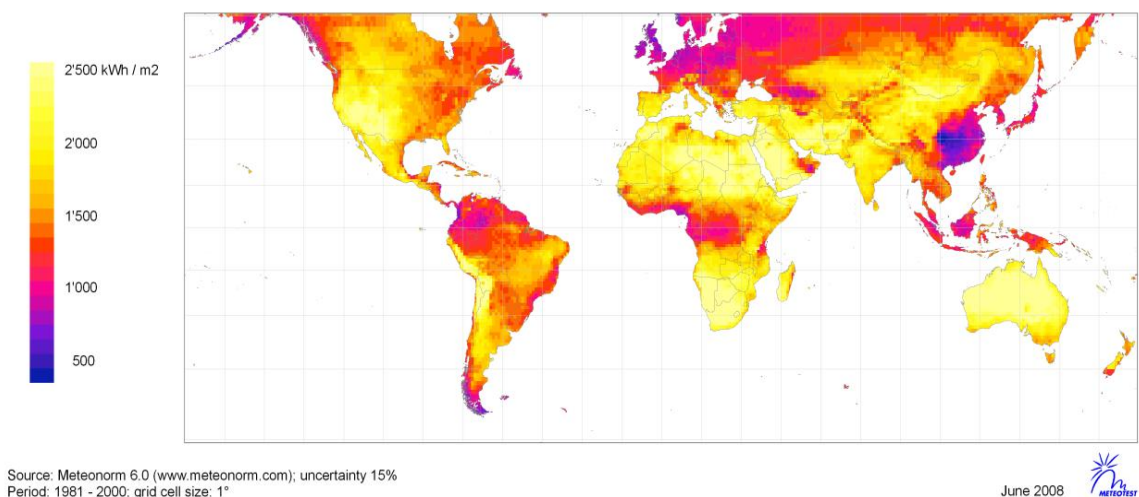


Figure 1.4: Yearly sum of direct beam insolation in the world

The average power density of solar radiation is 100-300 watts a square meter. The net conversion efficiency of solar electric power systems (sunlight to electricity) is typically 10-15 percent. So substantial areas are required to capture and convert significant amounts of solar energy to fulfill energy needs (especially in industrialized countries, relative to today's energy consumption). For instance, at a plant efficiency of 10 percent, an area of 3-10 square kilometers is required to generate an average of 100 megawatts of electricity-0.9 terawatt-hours of electricity or 3.2 pet joules of electricity a year using a photovoltaic system.

The PV electrification could be using the decentralized stand alone and centralized systems depending to the nature of the load and the distribution of houses. Photovoltaic electrification is limitedly used in different rural areas in Palestine mainly for schools, clinics, Bedouins communities, agricultural and animal farms, and private homes. The total installed capacity is about to 50kWp.

The policy of PV electrification focuses on settling the communities threatened from land confiscation and people eviction due to occupation practices especially after construction of the separation wall. It is urgently needed to enhance the living conditions of these communities by offering more and better quality services and implementing sustainable

development plans. The policy contributes to development of renewable energy resources and reliance reduction on imported fuels, and eventually leads to environment protection and sustainable development in the region.

The most recently PV electrification project was implemented by the energy research center at An Najah National University. It's about electrifying a Palestinian village Atouf by PV centralized power system. The village includes 25 houses, school, and clinic with power capacity about 24 kWp. The project is considered a successful renewable energy application in Palestine. The project was financed by EU. Another Project shown in Figure 1.5 for street lighting and electrification of public sites at Jib Aldeeb community is going to be implemented by Arijl institution. This project is financed by UNDP/PAPP, GEF and SGP [2].

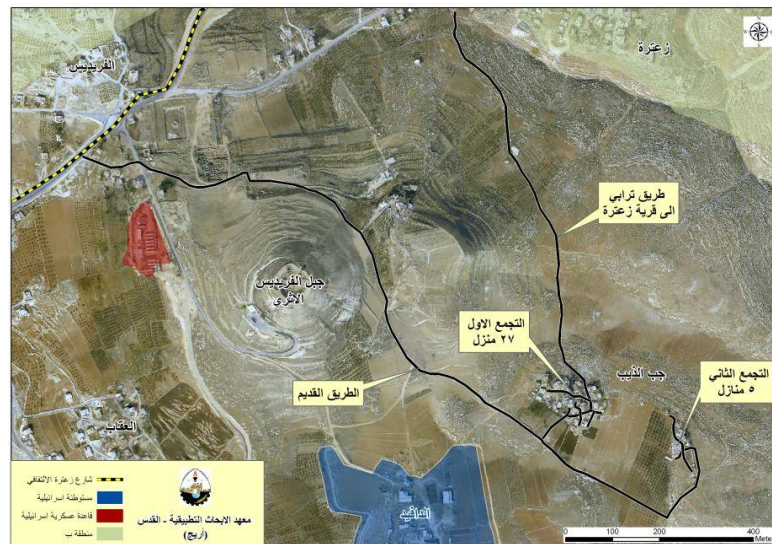


Figure 1.5: Solar street lighting of Jib Aldeeb Village in West Bank, Palestine

1.2 Research Motivation and Goal

According to the Political situation on Gaza Strip and the mandatory siege since 2006 by the Israeli occupation after Palestinian election, Power Generation Sector faced several obstacles starting with destroying main generators of Gaza Power Plant in June 2006 through blocking fuel entry into Palestinian Territories in 2008 ending to unknown and horrible situation. So the need of alternative and urgent power source to supply hospitals and medical centers is very important issue especially in situation we live in Gaza Strip; imposed siege, shortage in fuel supplies, and increasing in the mortality rate.

The most significant factors in designing of PV systems are cost-effectiveness and maximum power utilization. In most cases, PV Systems can compete with systems employing traditional energy resources if a life-cycle cost analysis is developed for a reasonable long period of time (approximately 25 years).

Although Palestinian Territories got a relatively abundant solar radiation, but it is not utilized in a good matter, some of renewable energy projects established in Palestine, such as “Using Solar Energy in Lighting the Beach Bridge in Gaza Village” which established in 2006. Some problems and drawbacks on the previous design such as the orientation and direction of PV modules, Controllers, Batteries, and Safety were noticed by Consultants. So the aim of this research is focusing on the design and methodologies that have been considered by designers, and make re-evaluation and re-design of the installed PV system.

According to my visit to the Authority of Energy in Gaza, and meeting the consultants of PV Projects there, they provided me with all required documents of previous projects, their notices, and recommendations as follows:

1.2.1 PV Modules

Unfortunately, all previous designs of Photovoltaic Projects in Gaza Strip done without any kind of survey for temperature degrees and irradiation, which affects on the orientation and direction of the PV module, and affect by the way on the absorbed irradiation and the converted power.

1.2.2 Controllers

All controllers used in the previous designs of PV projects in Gaza Strip are interested in Charge Controllers, the State Of charge (SOC) and Short/Open-circuit protection, but they don't include MPPT Controller with DC/DC Converter in order to get maximum power point in P-V Curve of PV module. Cell shading, variation of temperature and irradiation affect on the power absorbed by the PV system, so MPPT is needed to obtain the optimum solution.

1.2.3 Batteries

Batteries in PV system are needed when sunlight is unavailable. So the longest period without sunlight is an important factor in sizing batteries with considering cost effect. In the previous designs, batteries were not selected carefully to overcome the absence of sunlight.

1.2.4 Safety and Maintenance

Unfortunately, no safety and maintenance recommendations are considered in the previous designs, which affected on the performance of PV system. Uncertainty of electrical components according to aging and several factors could affect on the performance of PV system.

1.2.5 Cost versus Quality

The most important factor is the initial investment. These costs are high compared to other used energy. However, the costs over a life time are more favorable for PV because

no operating costs; the only costs after the installation are the maintenance costs. So the comparison should be made for a life time of PV system (20-25years). The better quality required for PV System, the higher cost should be paid.

The study on all previous lighting projects leads to several drawbacks on these projects, such as lack of meteorological information of Gaza Strip, Palestine, incorrect orientation and tilting plan, and insufficient both PV and Battery Sizing. So as a result, this research concentrates on the re-evaluation and re-design process for PV lighting projects in Gaza Strip, Palestine, this process is divided into four phases as shown in Figure 1.6



Figure 1.6: Re-Evaluation and Re-Design Process

A typical PV system consists of several PV Modules which consists of interconnection of $m \times n$ (*series* \times *parallel*) solar cells; those modules connected either in parallel and/or series topology based on the desired generated current and voltage respectively. PV Array connected to power interface consists of DC/DC Converter, DC/AC Inverter, and Charge Controller, and then they are connected to Loads as shown in

Figure 1.7.

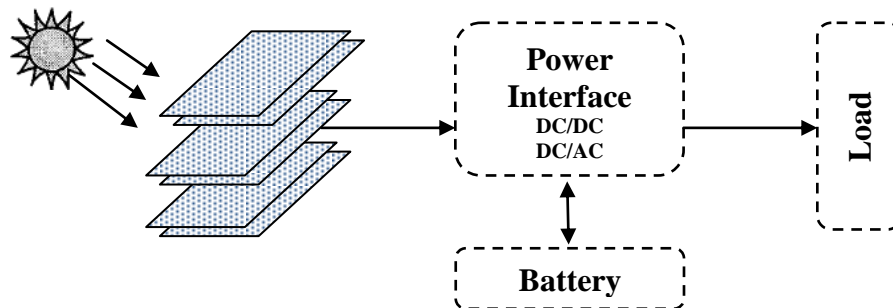


Figure 1.7: Typical PV System

1.3 Literature Review

1.3.1 Modeling of Global Radiation

Joakim Widén mentioned the models of solar radiation, daylight and solar cells as a chapter in his thesis [3]. He described the models implemented for calculating the daylight level and the power output from PV system, to be used in further simulations of domestic (Sweden) electricity demand, he gave a brief overview of models, then he described in his chapter how to determine incident radiation on a tilted plane from radiation components measured on a horizontal plane, then he described the daylight model and PV system model.

M.S.Alam et.al. developed a mathematical model for simulation of solar radiation system by using dynamics methodology in their paper [4]. Their model was developed for Bangladesh and their simulated results have been compared with the experimental results and found reasonably a good agreement. Therefore, the performance of their model is satisfactory and could be used in several locations with modifying some parameters.

1.3.2 Orientation and Tilt Angles

Danny Li et al. determined the optimum tilt angle and orientation for solar collection based on measured solar radiation data, his paper [5] presents a numerical approach to calculate the solar radiation on sloped planes by integrating the measured sky radiance distributions for Hong Kong.

Accordingly, his results showed that the solar radiation on a horizontal surface is around 1528kWh/m². The solar radiation rises with the tilt angle up to about 20° at which the maximum annual solar yield of 1598.4kWh/m² occurs. When the tilt angle is beyond 20°, the annual solar yield falls slightly with increasing tilt angles. As the latitude of Hong Kong is 22.3° N, the obtained results supports the argument that the optimal tilt angle for solar energy collection would be very close to the angle equivalent to the latitude of the location [5].

Jurgita and Mindaugas developed a new mathematical model of optimal tilt angles of solar collector and sunray reflector, their model [6] used to find the optimal tilt angle for both the solar collector (SC) and the Sunray reflector (SRR) for selected period of time. They found that there is an enhancement of the quantity of absorbed solar radiation by SC with SRR than those absorbed by SC only by (30 – 60) %.

D.Faiman et.al defined the “skewness” term in their paper [7], and shown the effect of miss orientation in BIPV by two case studies, one in SedeBoqer, Israel and the other case study was in Sydney, Australia. They found that annual beam energy gains of about 13% if collector skewness is correctly taken into account in the design of the system.

Emanuele found in his paper [8] a relationship between the optimum tilt angle and the geographic latitude. Furthermore, he found that the optimum tilt angle values for winter months were very different than those relative to summer months, so he suggested the idea of planning semi fixed solar panels.

1.3.3 PV System Model

Tasi et.al implemented a generalized photovoltaic model using Matlab/Simulink software package [9], which can be representative of PV cell, module, and array for easy use on simulation platform. Their proposed model is designed with a user-friendly icon and a dialog box like Simulink block libraries. His model will be helpful to develop similar model taking into account the variation of irradiation and temperature, also to be used in several power systems.

Dumitru et.al deals with the modeling of an electrical local network supplied with energy provided by renewable resources in their paper [10], their purpose is to implement and develop a software application to analyze and simulate a real hybrid solar-wind system connected to a local grid using Matlab /Simulink environment. Blocks like wind model, solar model, local grid model are implemented and the results of simulation were also presented. The main objective is the study of hybrid systems behavior, which allows employing renewable and variable in time energy sources while providing a continuous supply.

Weidong et.al proposed a novel model of PV system in their paper [11], which is able to demonstrate the cell's output features in terms of environment changes in irradiance and temperature. Based on a simplified single-diode model, the parameters are determined in the sense of minimum model error and temperature effect. Their model is tested to simulate three popular types of photovoltaic panels made of different materials, CIS thin film, multi-crystalline silicon, and mono-crystalline silicon. The effectiveness of their approach is evaluated through comparison of simulation results to the data provided by product's manufacturer.

1.3.4 PV Modules, Batteries, MPPT Controllers and Regulators

Esrarn et.al made a survey paper [12] on MPPT techniques; they discussed them, they shown that at least 19 distinct methods have been introduced in the literature, with many variations on implementation. Their paper should serve as a convenient reference for future work in PV systems, and the appropriate selection of MPPT techniques.

A New controller scheme for PV systems is proposed by Amin et.al in their paper [13], their scheme controls both the boost converter and battery charger by using a microcontroller in order to extract maximum power from the PV array and control the charging process of the battery, their objective was to present a cost effective boost converter design and an improved MPPT algorithm of PV system, their simulation results showed that the proposed boost converter gave a better converter efficiency about 93%.

Another technique used for MPPT by Orozco et.al. in their paper [14] using sliding mode control, their designed controller regulates the converter output voltage and maximize the power generated by the photovoltaic array, they proposed a sliding surface to control the dc/dc converter which is adjusted according to PV array output power. The results in a simulation platform were confirmed the adequate performance of designed control.

Song Kim et.al. present in their paper [15] the method to estimate the battery internal status such as SOC, terminal voltage and charging current, these estimated states could be used as a second protection method, the simulated results verified the performance of the proposed system, the merits of their proposed methods were simple structure with reduced sensors.

Supratim et.al described in their paper [16] a simple yet novel modification to the charging circuit for the battery of a standalone PV system, which described with an implementation flow chart/algorithm. Their results showed the effectiveness of their algorithm, compared to the traditional implementation.

1.3.5 Maintenance and Monitoring

Weidong et.al [17] looked at the performance of PV modules in non-ideal conditions and proposed topologies to minimize the degradation of performance caused by these conditions, they found that the peak power point of a module is significantly decreased due to only the slightest shading of the module, and this effect is propagated to the other non-shaded modules connected in series with the shaded one, their paper provides a comparative study to choose the right converter topology for the applications of dc/dc MPPT modules.

M. Hussein developed and implemented in his paper [18] an algorithm to obtain all possible vertex matrices for nxn interval matrix. He treated in his paper the uncertainty entries of a matrix, which is considered an important problem for control system engineers, especially on finding the eigenvalues to determine system stability, his simulation results showed the validation of his proposed algorithm. His algorithm could help us to study the stability of a PV system for uncertainty in electronic components due to aging.

1.4 Research Results and Contributions

This research is very useful for BIPV and Solar Energy Consultants who interest in Solar system design, Re-design and Re-Evaluation Process has been developed here step by step.

Developing an empirical global solar radiation model for Gaza Strip, Palestine and studying the suitable tilt angle and orientation, with feasibility study of one-axis two position manual tracks are considered main contributions to this research.

Candidates papers, which sent to the Journals, local and international conferences are accepted to be presented and published strength research.

1.5 Thesis Structure

There are six chapters in this thesis; Chapter 1 provides introduction and Literature review. Chapter 2 presents the first contribution of developing global solar radiation model for Gaza Strip, Palestine, with all derivation of the empirical model. Chapter 3 covers the suitable optimal orientation and tilt angle for Palestinian Territories, with mathematical derivation and developing new idea to enhance the performance. Chapter 4 focuses on the importance of battery and PV sizing in solar system design, with developing MATLAB software to help designers. Chapter 5 presents an experiment of lighting an apartment using solar energy. Finally in chapter 6, conclusion and recommendations for future work are given.

Chapter 2

Developing Empirical Models for Estimating Global Solar Radiation

2.1 Introduction

Palestine is located within the solar belt countries and considered as one of the highest solar potential energy, the climate conditions of the Palestinian Territories are predominantly very sunny with an average solar radiation on a horizontal surface about 5.4 kWh/m².day [19].

Gaza Strip is 360km² with a high density population of about 4,118 persons/km² [20], so Gaza Strip represents one of the most densely populated areas in The Middle East. As the population in Gaza Strip increases (population growth rate 3.349%/year [21]), the consumption of water and energy will increase; leading to significant rise in unacceptable levels of air pollution, and the defect in water supply and energy sources will increase; leading to severe economical crisis that will result in a significant rise in the probability of an outbreak of warfare.

So the need for renewable energy sources such as solar energy becomes essential trend especially in the political situation of Gaza Strip. The objective of this chapter to develop an empirical global solar radiation model using a simple meteorological data obtained from nearest centers of Gaza Strip.

2.2 Background

Understanding solar radiation data and the amount of solar energy intercepts specific area are essential for modeling solar energy system and covering the demand. Therefore, precise knowledge of historical global solar radiation at a location of study is required for the design of any funded solar energy project.

Unfortunately, no meteorological stations available in Gaza Strip to measure the amount of intercepted solar radiation in Gaza Strip. So an alternative method for estimation of solar radiation is required.

Several studies on modeling solar radiation have been done in Tunis [22], Bangladesh [4], Rwanda [23], Pakistan [24], and other developing countries. All of these studies used historical meteorological data of the location for estimating the empirical model. Empirical

models are classified into three categories: sunshine-based model, temperature-based model and cloud based models [23].

Sunshine based models are the most widely used, which use only bright sunshine hours as input parameter while others use additional meteorological data together with bright sunshine hours.

In this study, Angstrom-type polynomials of first and second order have been developed for estimating the global solar radiation in Gaza Strip, Palestine from a long term records of monthly mean daily sunshine hour values and measured daily global solar radiation on horizontal surface at several locations near Gaza strip or have the same climate conditions. The coefficients are derived by using least square regression analysis using MATLAB. These coefficients are generally valid for estimating the radiation in Gaza Strip, Palestine.

2.3 Methodology

The methodology used in this thesis consists of data gathering, description of model and the utilization and implementation of MATLAB as explained in the following sections:

2.3.1 Data:

In Gaza Strip, recorded global solar radiation data on horizontal surface were obtained from several stations around Gaza Strip as shown in Figure 2.1. According to [25] the solar radiation level for both areas Gaza Strip and Bet Dagan are similar.

Table 2.1 presents the location of stations and the period of observation for which global solar radiation H_g and sunshine duration L_h were measured.

Table 2.1: Location of stations and period of observation of global solar radiation

<i>Station</i>	<i>Altitude (ft)</i>	<i>Latitude (N)</i>	<i>Longitude (E)</i>	<i>H_g and L_h</i>
<i>Bet Dagan</i>	120	32° 00`	34° 49`	1991-2005
<i>Al-Arish^a</i>	75	31° 08`	33° 48`	1981-2000
<i>Rafah^b</i>	114	31° 17`	34° 14`	1981-2000
<i>BenGurion Airport^c</i>	145	32° 00`	34° 52`	1981-2000

a, b, c Records of these location are obtained using METEOTEST Software

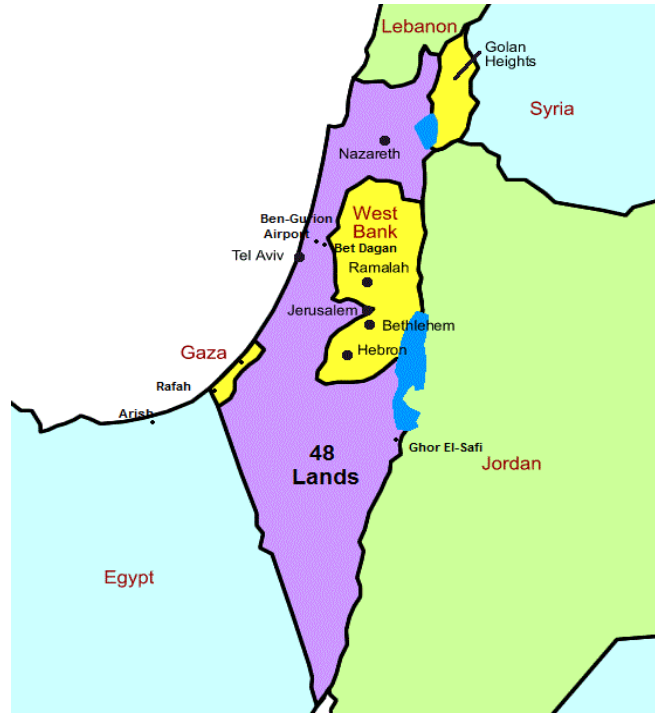


Figure 2.1: Location of Stations that record Global Solar Radiation

2.3.2 Description of the Model:

The model is based on 14 years of data (91-05) and 20 years of data (81-00) from Bet Dagan and METEOTEST Software respectively.

Angstrom's equation [26] is used to express the average radiation on a horizontal surface in terms of constants α_1, α_2 and the observed values of average length of solar days. The constants α_1, α_2 will be determined for this model based on actual old measurements and equating the data in the Angstrom's equation given as follows:

$$\frac{H_g}{H_c} = \alpha_1 + \alpha_2 \left(\frac{L_h}{L_m} \right) \quad (2.1)$$

Where

L_h is the average length of solar day for a given month calculated/observed.

L_m is the length of the longest day in the month.

α_1, α_2 are the average length of solar day for a given month calculated/observed.

H_g is the monthly average of daily global radiation on the horizontal surface at a particular location.

H_c is the maximum monthly average of daily global radiation per day corresponding to clear sky

Values of L_m or Day Length (DL) are computed from Cooper's formula [27] as follows:

$$L_m = \left(\frac{2}{15} \right) \omega_s \quad (2.2)$$

$$\omega_s = \cos^{-1}(-\tan \phi \tan \delta) \quad (2.3)$$

Where

ω_s is the Sunshine Hour Angle

ϕ is the latitude of the location. ($31^\circ 27'$ for Gaza)

δ is the solar declination angle, which defined as the angle between the line joining centers of the sun and earth and the equatorial plane.

Values of δ are computed from the following relation [26],

$$\delta = 23.45 \sin \left(\frac{360 (284 + n)}{365} \right) \quad (2.4)$$

Where

n is the day of the year, it is usually calculated in the 15th of each month.

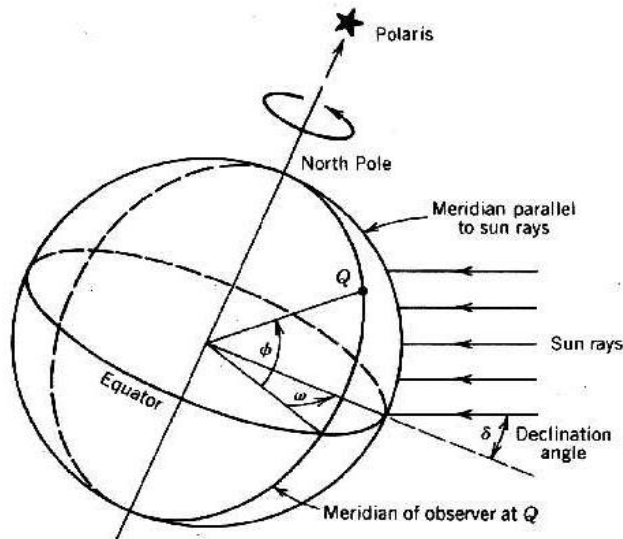


Figure 2.2: Earth-Sun Angles; Latitude(ϕ), Declination Angle (δ) and Hour Angle (ω)

Back to equation (2.1), H_c is replaced with H_o according to changes done on modified Angstrom's Equation for Daily Global Radiation, where H_o is the Daily extra-terrestrial radiation, mean value for the month, which computed by the following relationship in [26]:

$$H_o = \frac{24}{\pi} I_{sc} \left(1 + 0.33 \cos \frac{360n}{365} \right) (\omega_s \sin \phi \sin \delta + \cos \phi \cos \delta \sin \omega_s) \quad (2.5)$$

Where

I_{sc} is the Solar Constant ($1353 \text{ kW/m}^2 = 4870.8 \text{ kJ/m}^2 \cdot \text{hr}$)

Using the data of Global Radiation H_g and the average length of solar day L_h around the location of Gaza Strip, the regression constants of Angstrom's Equation α_1, α_2 could be obtained using MATLAB.

The Second order polynomial of Angstrom's Equation developed in [24] is also used in this paper to be modeled for our case in Gaza Strip, Palestine.

$$\frac{H_g}{H_o} = \alpha_3 + \alpha_4 \left(\frac{L_h}{L_m} \right) + \alpha_5 \left(\frac{L_h}{L_m} \right)^2 \quad (2.6)$$

Where

$\alpha_3, \alpha_4, \alpha_5$ are the Angstrom's Constants

2.3.3 MATLAB Program:

The regression constants $\alpha_1, \alpha_2, \dots, \alpha_5$ have been obtained using a software computer program called MATLAB, the program employees the robust least square regression technique. Sum of Square Errors (SEE), Root Mean Square Error (RMSE), and Square of Correlation coefficients R^2 are calculated to assess the validity of estimation, and also to compare between two types of Angstrom's Equation.

2.4 Results and Discussion

Linear and polynomial least square regression techniques were implemented using the observed metrological data at Bet Dagan and METEOTEST Software as given in Table 2.2.

Figure 2.3 shows the clearness index for Gaza Strip, Palestine. The curve indicates that Gaza Strip has clear sky condition most of the year, and the clearness index has maximum values on Jun-Aug with maximum sunshine hours, which implies that the maximum utilization of solar energy will be in summer.

Table 2.2: Input Parameters for Angstrom's Equations

<i>Locat.</i>	<i>From Equ. (2.2), (2.5)</i>		<i>Bet Dagan</i>	<i>METEO-TEST</i>	<i>Average of Observed Values</i>	
<i>Month</i>	H_o	L_m (hrs)	H_g	H_g	H_{avg} (kWh/m ² .d)	L_h (hrs)
Jan	7.05	10.79	2.61	3.24	2.9240	6
Feb	8.16	11.27	3.4	4.01	3.7035	7
Mar	9.36	11.85	4.7	5.32	5.0086	7.5
Apr	10.39	12.51	5.86	6.34	6.1019	9
May	10.87	13.05	6.88	7.20	7.0417	10.5
Jun	10.98	13.34	7.55	7.65	7.6014	12
Jul	10.9	13.22	7.29	7.80	7.5458	12
Aug	10.55	12.76	6.67	7.16	6.9133	11.5
Sept	9.73	12.12	5.69	6.29	5.9922	10
Oct	8.52	11.48	4.25	4.94	4.5964	9
Nov	7.31	10.92	3.09	3.89	3.4922	7
Dec	6.73	10.66	2.48	3.03	2.7525	6

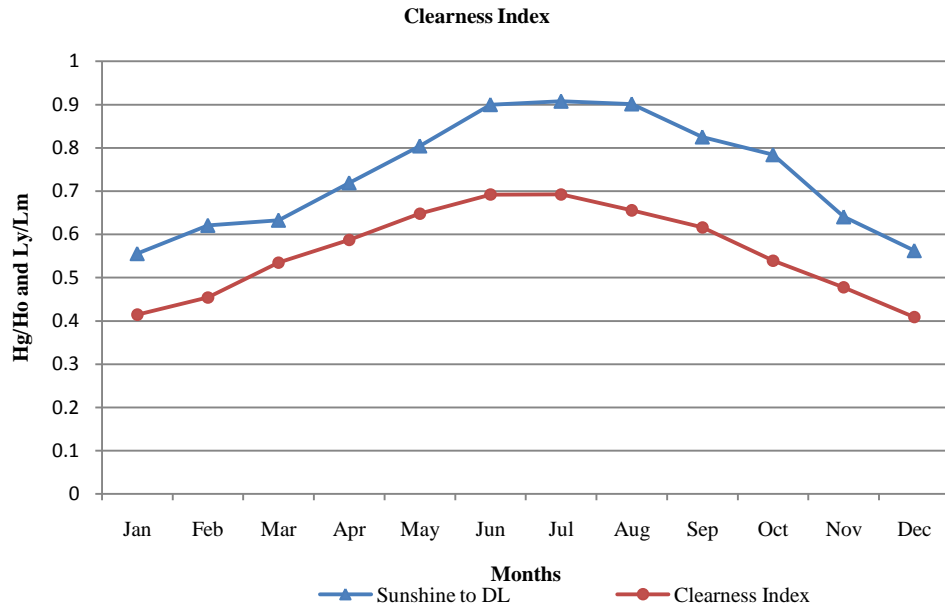


Figure 2.3: The Clearness Index for Gaza Strip, Palestine

The computed values for regression coefficients are

$$\alpha_1 = -0.002351, \alpha_2 = 0.7607, \alpha_3 = -0.3941, \alpha_4 = 1.868, \alpha_5 = -0.7551.$$

So the first and second order Angstrom's Equation are then given respectively by:

$$\frac{H_g}{H_o} = -0.002351 + 0.7607 \left(\frac{L_h}{L_m} \right) \quad (2.7)$$

$$\frac{H_g}{H_o} = -0.3941 + 1.868 \left(\frac{L_h}{L_m} \right) - 0.7551 \left(\frac{L_h}{L_m} \right)^2 \quad (2.8)$$

The comparison between the estimated values using the previous equations (2.7) and (2.8) respectively, with the observed values are given in Table 2.3

Table 2.3: Comparison between the observed and estimated global solar radiation for Gaza Strip

<i>Locat.</i>	<i>Estimated</i> <i>H_g (kWh/m².d)</i>		<i>Observed</i> <i>H_g (kWh/m².d)</i>		<i>Old</i> <i>Model</i>
	<i>Linear</i>	<i>Polyn.</i>	<i>Bet</i> <i>Dagan</i>	<i>METEO-</i> <i>TEST</i>	<i>Gaza</i> <i>Station</i>
<i>Jan</i>	2.9660	2.8986	2.61	3.24	2.70
<i>Feb</i>	3.8345	3.8729	3.4	4.01	3.12
<i>Mar</i>	4.4872	4.5492	4.7	5.32	3.67
<i>Apr</i>	5.6604	5.8064	5.86	6.34	4.25
<i>May</i>	6.6238	6.7365	6.88	7.20	4.87
<i>Jun</i>	7.4911	7.4170	7.55	7.65	5.27
<i>Jul</i>	7.4984	7.4029	7.29	7.80	5.35
<i>Aug</i>	7.2059	7.1305	6.67	7.16	5.18
<i>Sept</i>	6.0819	6.1579	5.69	6.29	4.67
<i>Oct</i>	5.0650	5.1693	4.25	4.94	3.87
<i>Nov</i>	3.5474	3.6040	3.09	3.89	2.94
<i>Dec</i>	2.8660	2.8138	2.48	3.03	2.61

Figure 2.4 shows the small difference between the estimated and the observed values, while the old model of Gaza Station [28] has a huge gap between their results and the results of the developed model. Also there is a difference between their model and the observed data of Bet Dagan itself, where they used its metrological data for modeling.

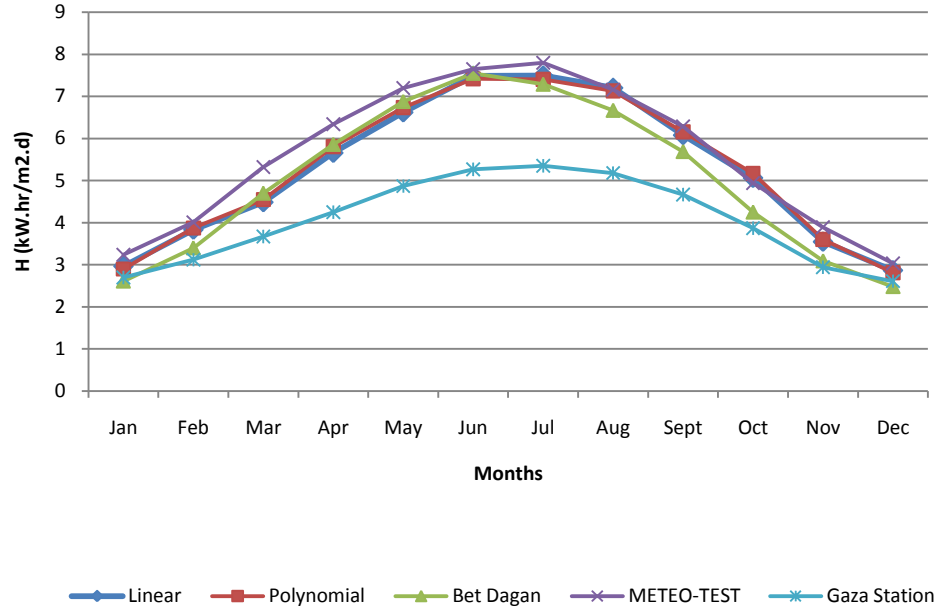


Figure 2.4: Comparison between the estimated and the observed values

The deviations between the estimated values of the developed model and the observed global solar radiation data are given in Table 2.4, SSE, R2 and RMSE are calculated using the equations and formulas found in [29].

As shown in Table 2.4, the linear model has the best results when compared with Bet Dagan Station; while the polynomial model has the best results when compared with METEOTEST Station. Both models have fine agreement between measured and estimated values.

Both linear and polynomial models are not suitable for Old Gaza station model, which indicates that low accuracy of that model.

Table 2.4: Deviations between the estimated model and the observed global solar radiation data

<i>Data</i>	<i>Developed Model</i>	<i>SSE</i>	<i>R²</i>	<i>RMSE</i>
<i>Bet Dagan</i>	<i>Linear</i>	1.9764	0.9492	0.4058
	<i>Polynomial</i>	2.0353	0.9478	0.4118
<i>Meteo-Test</i>	<i>Linear</i>	1.9148	0.9441	0.3995
	<i>Polynomial</i>	1.6405	0.9519	0.3697
<i>Old Gaza Model</i>	<i>Linear</i>	23.8233	0.2070	1.4090
	<i>Polynomial</i>	24.2984	0.2064	1.4230

As a result, the developed Angstrom's Equations, both first and second order type could be simply applied to estimate monthly average daily global radiation from monthly average daily sunshine hours, which are available in primary station across Gaza Strip, Palestine.

2.5 Conclusion

The development of the Angstrom's Equation for Gaza Strip, Palestine is considered in this study, both types of linear and polynomial type have been developed and tested to measure the fine agreement between the observed and estimated values. From the comparison of these results, it was observed that the estimated values of both models were in a good agreement with both observed values from Bet Dagan and METEOTEST Stations, which strengthen the developed model, and could be easily applied to Gaza Strip, Palestine.

Chapter 3

Optimum Tilt Angle & Orientation for PV Panels

3.1 Introduction

Orientation of solar collector (SC) in space is the main factor influencing the quantity of absorbed solar radiation energy. In the case with optimal angles of a solar collector, we will have the maximum of solar radiant energy.

The optimal angles depend on the geographical position and on the investigation period (day, week, month, etc.) when the position of a solar collector will be stationary. It is very important, because the trajectory of the sun changes. The intensity of solar radiation energy, sunlight duration per day and per year change as well.

Conventionally, stand-alone PV systems have been used in rural and remote areas where normal electricity supply may not be readily accessible. In modern urban cities with many compactly built high-rise blocks, the concept of building integrated photovoltaic (BIPV) would be an appropriate alternative form to receive solar energy [30]. In designing the optimal tilt angle and orientation of a fixed solar panel for maximizing its energy collection is to acquire the maximum solar radiation availability at the required location, a number of studies have been conducted by various researchers to determine the optimum location for solar radiation collection using different empirical models [31].

One of the objectives of this research is to provide technical information about tilt angle and orientation of PV Panels for both Architects who interests in Building-Integrated Photovoltaic (BIPV) applications and Practitioner Engineers who interests in the utilization of renewable energy in Gaza Strip, Palestine to improve and enhance the efficiency of PV System used in their designs with reduced cost.

3.2 Earth –Sun Geometry

The term Earth rotation refers to the spinning of our planet on its axis. Because of rotation, the Earth's surface moves at the equator at a speed of about 467 m per second or slightly over 1675 km per hour. One rotation takes exactly twenty-four hours and is called a mean solar day. The Earth's rotation is responsible for the daily cycles of day and night. At any one moment in time, one half of the Earth is in sunlight, while the other half is in darkness.

The edge dividing the daylight from night is called the circle of illumination. The Earth's rotation also creates the apparent movement of the Sun across the horizon.

The orbit of the Earth around the Sun is called an Earth revolution. This celestial motion takes 365.26 days to complete one cycle. Further, the Earth's orbit around the Sun is not circular, but oval or elliptical. An elliptical orbit causes the Earth's distance from the Sun to vary over a year. Yet, this phenomenon is not responsible for the Earth's seasons. This variation in the distance from the Sun causes the amount of solar radiation received by the Earth to annually vary by about 6%. Figure 3.1 illustrates the positions in the Earth's revolution where it is closest and farthest from the Sun. On January 3, perihelion, the Earth is closest to the Sun (147.3 million km). The Earth is farthest from the Sun on July 4, or aphelion (152.1 million km). The average distance of the Earth from the Sun over a one-year period is about 149.6 million km [32].

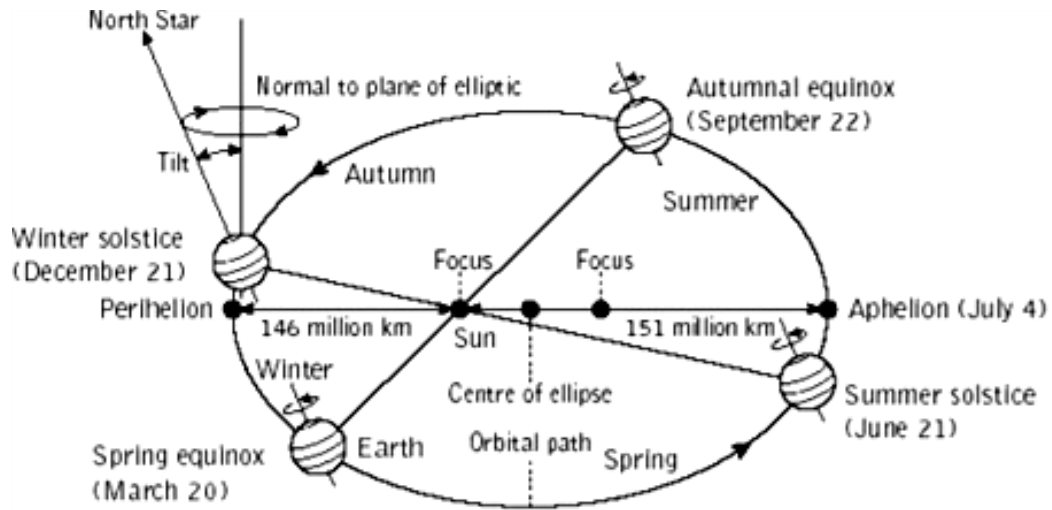


Figure 3.1: Earth Revolution around Sun

The annual change in the relative position of the Earth's axis in relationship to the Sun causes the height of the Sun or solar altitude to vary in our skies. Solar altitude is normally measured from either the southern or northern point along the horizon and begins at zero degrees. Maximum solar altitude occurs when the Sun is directly overhead and has a value of 90°. The total variation in maximum solar altitude for any location on the Earth over a one-year period is 47° (Earth's tilt 23.5° x 2 = 47°). This variation is due to the annual changes in the relative position of the Earth to the Sun. At 50 degrees North, maximum solar altitude varies from 63.5 degrees on the June solstice to 16.5 degrees on the December solstice. At our case in Gaza Strip, maximum solar altitude varies from 80 degrees on the June solstice to 33 degrees on the December as shown in Figure 3.2.

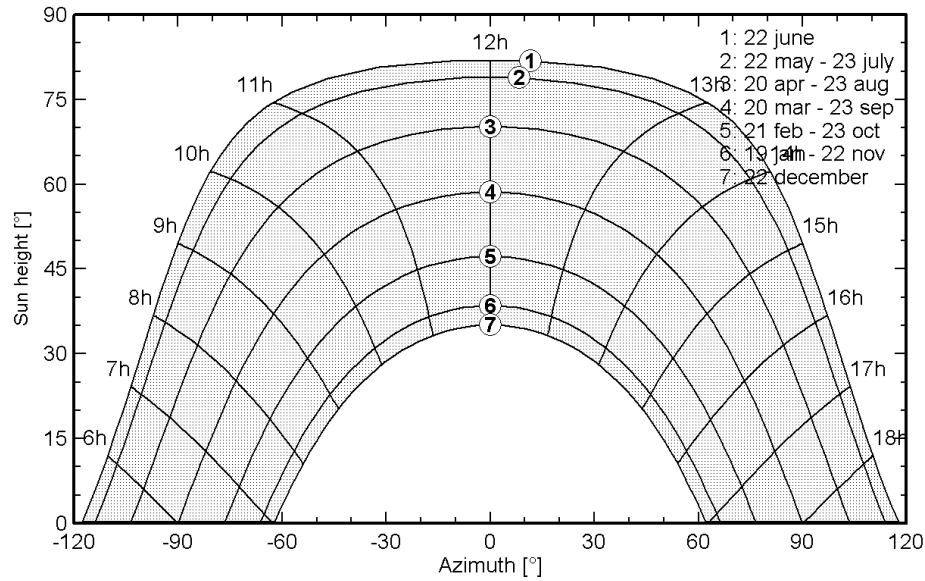


Figure 3.2: Sun path at Gaza along the year

3.3 Methodology and Design

3.3.1 Definition of Angles:

3.3.1.1 Earth-Sun Angles

The Hour Angle (ω): Angular displacement of the sun east or west of the local meridian due to rotation of the earth on its axis at 15° per hour as shown in Figure 3.1. The hour angle is variable within the day, negative for morning, positive for afternoon and zero at solar noon as shown in Figure 3.3. It can be expressed by

$$\omega = 15(t - 12) \quad (3.1)$$

Where

ω is the hour angle in degrees

t is the solar time in hours.

The Declination Angle (δ): Angle made between the line drawn joining the center of the earth and the sun and the earth's equatorial plane. It is zero at the autumnal and vernal equinoxes. The range of declination angle is given by $-23.45^\circ \leq \delta \leq 23.45^\circ$ as shown in Figure 3.4.

$$\delta = 23.45 \sin \left(360 \frac{(284 + n)}{365} \right) \quad (3.2)$$

Where

δ is the declination angle in degrees

n is the day number.

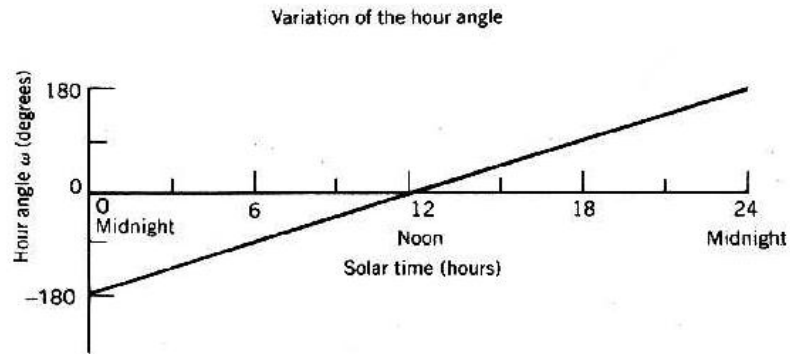


Figure 3.3: Variation of Hour Angle

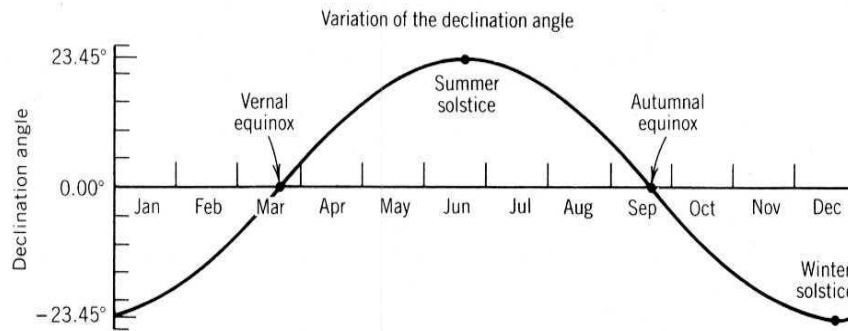


Figure 3.4: Variation of Declination Angle

Latitude (φ): Angular distance of the point on the earth measured north or south of the equator as shown in Figure 2.2, its values between $-90^\circ \leq \varphi \leq 90^\circ$

3.3.1.2 Observer-Sun Angles

Solar Altitude Angle (α_s): it is the angle between the projection of the sun's rays on the horizontal plane and the direction of the sun's rays as shown in Figure 3.5.

Solar Zenith Angle (θ_s): it is the complement angle of Altitude Angle as shown in Figure 3.5.

$$\theta_s = 90 - \alpha_s \quad (3.3)$$

Solar Azimuth Angle (γ_s): it is the angle measured clockwise on the horizontal plane from the north-pointing coordinate axis to the projection of the sun's ray.

3.3.2 Derivation of Solar Angle $\cos\theta_s(\sin\alpha_s)$:

The effective solar insolation that intersects the fixed solar plate depends on the solar angle $\cos\theta_s(\sin\alpha_s)$, which will be derived in this section.

3.3.2.1 Fixed Horizontal Plate:

Assuming the solar radiation vector according to earth surface coordinate is $S = SR_Z i + SR_E j + SR_N k$, and the same vector according to space coordinate is $S = SR_m i + SR_e j + SR_p k$, so as shown in Figure 3.5, the (zen \approx xyz) coordinates describe the location of the solar panel on the earth surface, assuming the panel is horizontal and faced to south, so the coordinate should be rotated about the east axis by latitude angle φ as follows:

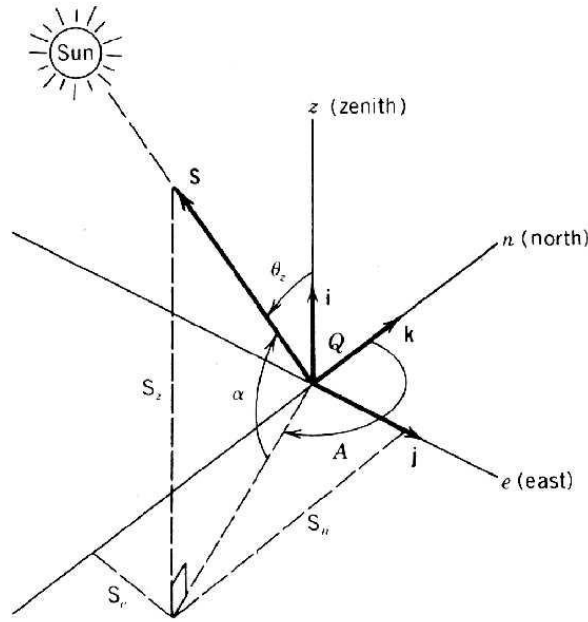


Figure 3.5: Earth Surface coordinate system for observer

$$\begin{bmatrix} SR_Z \\ SR_E \\ SR_N \end{bmatrix} = \begin{bmatrix} C_\varphi & 0 & S_\varphi \\ 0 & 1 & 0 \\ -S_\varphi & 0 & C_\varphi \end{bmatrix} \begin{bmatrix} SR_m \\ SR_e \\ SR_p \end{bmatrix} \quad (3.4)$$

Where

$$\begin{bmatrix} SR_m \\ SR_e \\ SR_p \end{bmatrix} = \begin{bmatrix} C_\delta C_\omega \\ C_\delta S_\omega \\ S_\delta \end{bmatrix} \quad (3.5)$$

Notice that C_X stands for $\cos X$, and S_X stands for $\sin X$.

3.3.2.2 Fixed Tilted Plate:

In case the plate should be tilted by angle β and faced to south by angle γ as shown in Figure 3.6, so the previous coordinate should be rotated about the zenith axis by angle γ , followed by rotation about the east axis by angle β as follows:

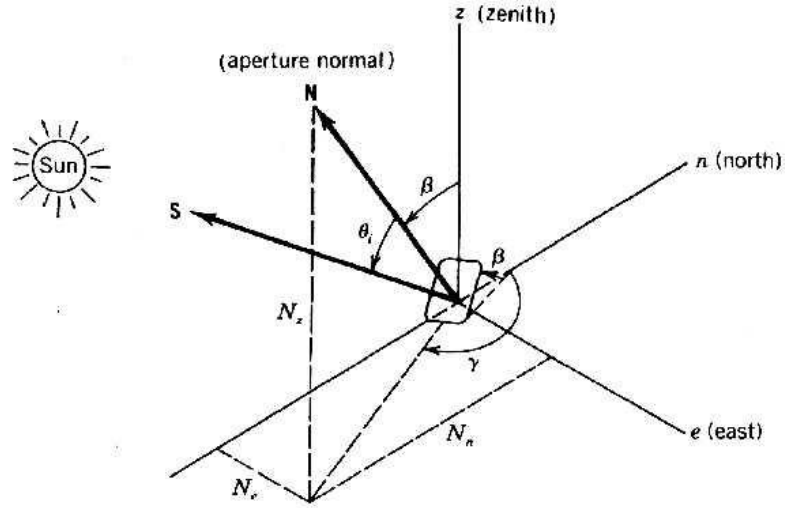


Figure 3.6: Earth Surface coordinate system for tilted observer

$$\begin{bmatrix} NR_Z \\ NR_E \\ NR_N \end{bmatrix} = \begin{bmatrix} 1 & 0 & 0 \\ 0 & C_\gamma & S_\gamma \\ 0 & -S_\gamma & C_\gamma \end{bmatrix} \begin{bmatrix} C_\beta & 0 & S_\beta \\ 0 & 1 & 0 \\ -S_\beta & 0 & C_\beta \end{bmatrix} \begin{bmatrix} SR_Z \\ SR_E \\ SR_N \end{bmatrix} \quad (3.6)$$

Where

$$\begin{bmatrix} NR_Z \\ NR_E \\ NR_N \end{bmatrix} = \begin{bmatrix} S_{\alpha_s} \\ C_{\alpha_s} S_{\gamma_s} \\ C_{\alpha_s} C_{\gamma_s} \end{bmatrix} \quad (3.7)$$

The Solar Angle S_{α_s} is derived from the previous equations (3.4-3.7) in terms of earth-sun angles as follows:

$$S_{\alpha_s} = C_\beta (S_\delta S_\varphi + C_\delta C_\varphi C_\omega) - C_\delta S_\omega S_\beta S_\gamma + S_\beta C_\gamma (S_\delta C_\varphi - C_\delta C_\omega S_\varphi) \quad (3.8)$$

3.3.3 Derivation the Optimum Tilt and Azimuth angles for the Solar Plate:

This section is dealing with the major components of the proposed mentioned design model, those major components are derived using mathematical equations as described in the following sections:

3.3.3.1 Optimum Azimuth angle:

By taking the first derivative of the previous equation (3.8) relative to variable γ , the equation will be as follows:

$$\frac{dS_{\alpha_s}}{d\gamma} = -C_{\delta}S_{\omega}S_{\beta}C_{\gamma} - S_{\beta}S_{\gamma}(S_{\delta}C_{\varphi} - C_{\delta}C_{\omega}S_{\varphi}) = 0 \quad (3.9)$$

Implies that

$$\tan \gamma_{opt} = \frac{-C_{\delta}S_{\omega}}{(S_{\delta}C_{\varphi} - C_{\delta}C_{\omega}S_{\varphi})} \quad (3.10)$$

Since the maximum insolation occurred at noon, so we could substitute $\omega = 0$ in the previous equation (3.10) to obtain the optimum azimuth angle as follows:

$$\gamma_{opt} = 0^{\circ} \text{ or } 180^{\circ} \quad (3.11)$$

3.3.3.2 Optimum Tilt angle:

By taking the first derivative of equation (3.8) relative to variable β , the equation will be as follows:

$$\begin{aligned} \frac{dS_{\alpha_s}}{d\beta} = & -S_{\beta}(S_{\delta}S_{\varphi} + C_{\delta}C_{\varphi}C_{\omega}) - C_{\delta}S_{\omega}C_{\beta}S_{\gamma} \\ & + C_{\beta}C_{\gamma}(S_{\delta}C_{\varphi} - C_{\delta}C_{\omega}S_{\varphi}) = 0 \end{aligned} \quad (3.12)$$

For simplicity, assume that $\gamma = \gamma_{opt} = 0^{\circ}$ and $\omega = \omega_{noon} = 0^{\circ}$, so the equation (3.12) is reduced to

$$\begin{aligned} \frac{dS_{\alpha_s}}{d\beta} = & -S_{\beta}(S_{\delta}S_{\varphi} + C_{\delta}C_{\varphi}) + C_{\beta}(S_{\delta}C_{\varphi} - C_{\delta}S_{\varphi}) \\ = & S_{\delta}(C_{\beta}C_{\varphi} - S_{\beta}S_{\varphi}) - C_{\delta}(S_{\beta}C_{\varphi} + C_{\beta}S_{\varphi}) \\ = & S_{\delta}C_{(\beta+\varphi)} - C_{\delta}S_{(\beta+\varphi)} = 0 \end{aligned} \quad (3.13)$$

Implies that

$$\beta_{opt} = \delta - \varphi \quad (3.14)$$

Figure 3.7 shows the optimum tilt angle curve along the year, in winter, the tilt angle approaches to 55° , while in summer it approaches to 8° . Assuming all previous angles are random variables, so the expected values for those variables as follows:

$$E[\beta_{opt}] = E[\delta] - E[\varphi] \quad (3.15)$$

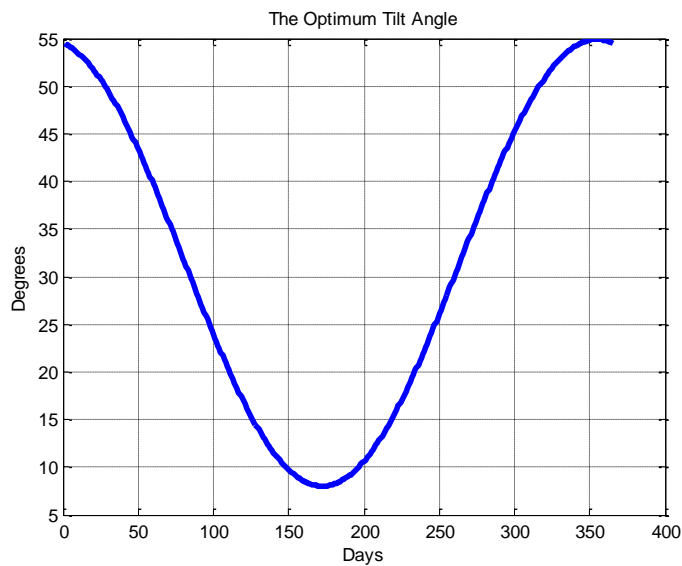


Figure 3.7: The Optimum Tilt Angle along the year

Since the declination angle acts as sinusoidal wave, so its expected value equals Zero, which implies the average optimum tilt angle should equal the latitude of the location as follows:

$$E[\beta_{opt}] = \varphi \quad (3.16)$$

3.3.4 Computing the Solar Angle $\cos\theta_s$:

Substituting the optimum values of Azimuth and Tilt angles in equation (3.8) to obtain the following curve in Figure 3.8.

Random selection of PV orientation (tilt and azimuth angles) is generated by MATLAB simulation, the mean value for the solar angle along is computed for each record. The maximum mean value for the solar angle along the year is 0.9586 found at the derived optimum orientation as shown in Table 3.1.

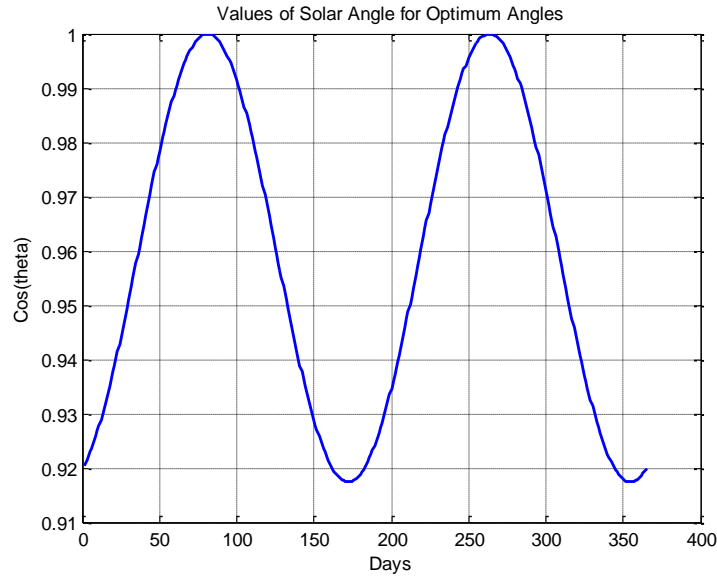


Figure 3.8: Values of Solar Angles in Degree for Optimum Tilt & Azimuth Angles

Table 3.1: Mean values of solar angles for different tilt and azimuth angles by MATLAB Simultaion

<i>Tilt Angles</i>	<i>Azimuth Angles</i>	<i>Mean Value of Solar Angle</i>
55	150	0.8239
8	20	0.7442
45	220	0.8492
28	40	0.5420
50	70	0.3945
13	180	0.9092
25	140	0.9030
50	90	0.5256
35	140	0.8896
31.464	180	0.9586

3.3.5 Enhancement on the Optimum Values:

Several studies such as [32] and [33] proposed new designs to enhance the solar power of PV Systems, Abu Hanieh [32] has shown theoretically that for Palestinian Territories, compared to a fixed PV module tilted at an angle equal to the local latitude, the power

generation can be increased by 40% using two axis tracking. He found the feasibility of two degree of freedom orientation and can be done utilizing part of the power output of the solar panel.

Another solution toward cost reduction is [33] to use the proposed idea of one axis three position tracking PV module with low concentration ratio reflector to provide a simpler PV tracking system. Their analysis shows that the power generation can be increased further by about 23% using a low concentration (2X) reflector in addition to the power output increase of 24.5% by using one axis three position tracking. Combining both, the total increase in power generation is about 56%.

In this research, we propose a new idea of one axis two positions tracking PV module without any controllers (manually) to provide costless PV tracking system and to enhance the efficiency of generated power.

Two factors are considered in this design; the solar insolation along the year and the solar angle. Figure 3.9 depicts the empirical models for global solar radiation in Gaza Strip along the year [34], the global solar radiation is increased to maximum ($> 7 \text{ kWh/m}^2$) in summer season (May-August), while the solar angle is decreased to minimum in the same season as shown in Figure 3.8.

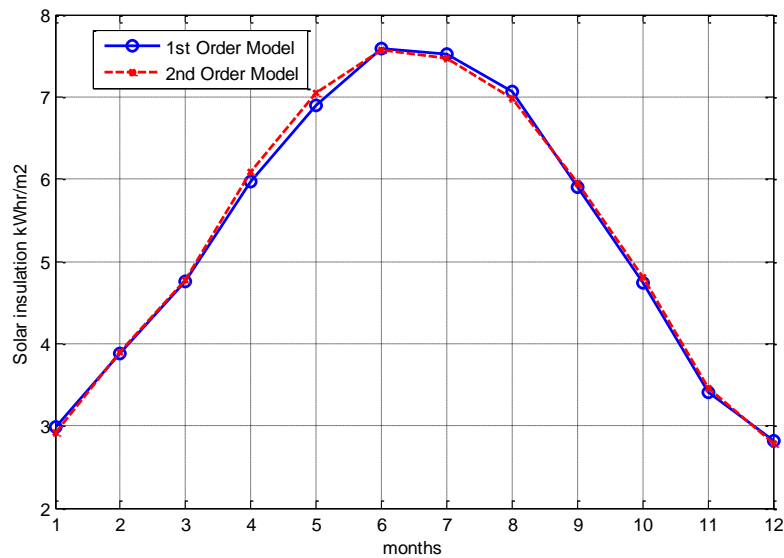


Figure 3.9: Empirical Models developed by Al Barqouni and Hussein

The need of one axis two positions manually tracking PV system is declared here, which could be performed using PV panel with adjustable gear as shown in Figure 3.10 to meet variation in tilt angle. Tilt angle will be switched twice a year in the proposed idea (at the beginning and the end of summer season).

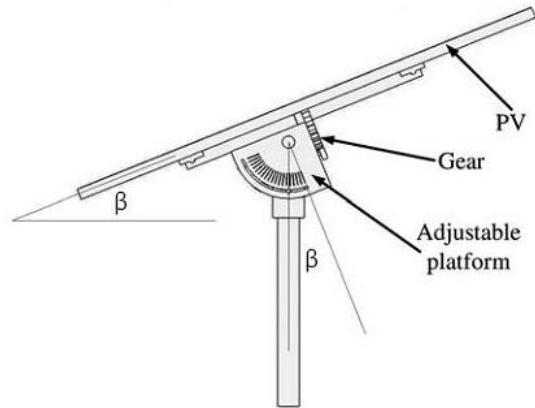


Figure 3.10: PV Panels supported with adjustable gear

3.4 Implementation

Unfortunately, all previous projects done in Gaza Strip related to solar energy done without any technical design for obtaining the maximum solar energy.

In this case, the project of Lighting Gaza Valley Bridge is discussed here. The solar panels used in the project are fixed with tilt angle 45° as shown in Figure 3.11.



Figure 3.11: Fixed Solar Panels for Lighting Gaza Valley Bridge

The Solar panels fixed with azimuth angle of 220° along with Gaza Valley Street as shown in Figure 3.12.



Figure 3.12: Gaza Valley Way Map by Google Earth®

When we compute the solar angle along the year for the given angles of the previous design, we obtain the dashed curve as shown in Figure 3., while the solid curve depicts the solar angle for the optimum orientation ($\beta_{opt} = 31.464^\circ$, $\gamma_{opt} = 180^\circ$).

Table 3.2 shows the difference between both orientations, while there is an improvement by 13% of the previous design.

Table 3.2: Comparison between current and optimum orientation

<i>Orientation</i>	<i>Tilt Angles</i>	<i>Azimuth Angles</i>	<i>Mean Value of Solar Angle</i>
Current	45	220	0.8492
Optimum	31.464	180	0.9586
Improvement			12.88%

Figure 3.13 shows the difference between the current and optimal orientation, while Figure 3.14 shows the enhancement in the solar angle when the proposed idea has been applied and the tilt angle has been adjusted to 13° at the beginning of summer (104th day) and re-adjusted again to 31.464° at the end of summer (240th day).

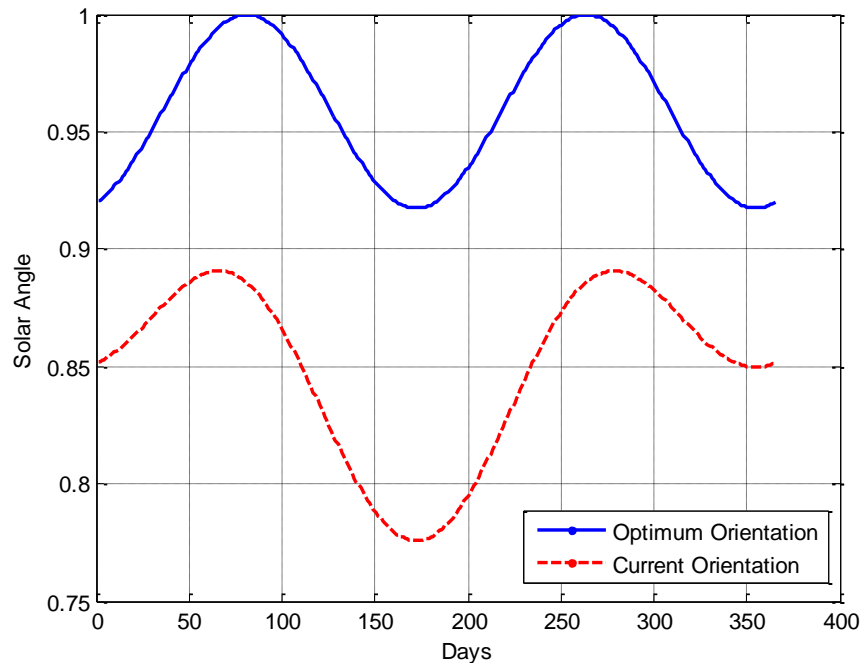


Figure 3.13: Current Orientation Vs. Optimum Orientation

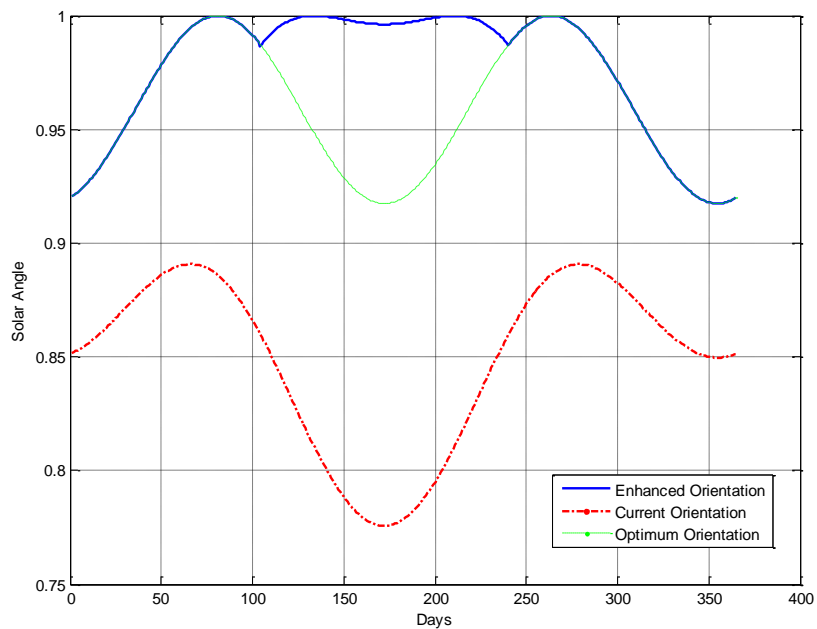


Figure 3.14: Enhanced Orientation Vs. Optimum Orientation

Table 3.3: Comparison between various orientations

<i>Orientation</i>	<i>Tilt Angles</i>	<i>Azimuth Angles</i>	<i>Mean Value of Solar Angle</i>
Current	45	220	0.8492
Optimum	31.464	180	0.9586
Enhanced	31.464, 13	180	0.9777
Current to Enhanced Improvement	17.0861 %	Optimum to Enhanced Improvement	2.7147 %

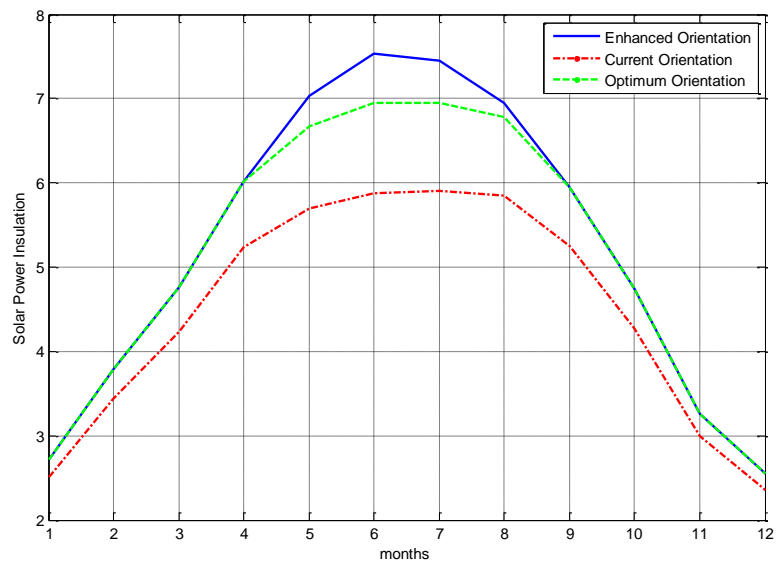


Figure 3.15: Improvement in Solar Power Insolation

Table 3.3 shows the comparison between various settings of orientation and tilting; the performance would be better when the mean value of solar angle approaches to 100%.

The Solar Power Insolation is computed for each setting as depicted in Figure 3.15. As shown, the enhanced model of orientation setting is similar to the developed empirical model in Figure 3.9.

3.5 Discussion & Conclusion

Researchers derived the optimum tilt and azimuth angles for PV module using mathematical equations; they found the optimum azimuth angle is 180° facing to south, and the optimum tilt angle is the geographical latitude of Gaza Strip 31.464° .

A new design idea of one axis two position manual tracking PV module was proposed in this thesis, a design analysis was performed for the enhanced model and the results show that the power generation can be increased by 17% of the previous design, and can be increased by 3% of the optimum design without any additional cost.

The results obtained in this research could be used as guidance for PV System installers in future; the results would be enhanced by using both Solar Concentrator (SC) plates with Solar Panels and Two Axis Automatic Tracking System, where the main idea in this research, how to enhance the previous project and put it on the right way, without any additional equipments.

Researchers strongly recommend their design to be used in BIPV and Lighting Projects in Palestinian Territories; they proposed two positions tracking for simplicity, and to meet maintenance requirements of solar panels.

Chapter 4

PV System Components: PV Modules, Batteries and Charge Controllers

4.1 Introduction

The major aspects in the design of PV system are the reliable power supply of the consumer under varying atmospheric conditions and the corresponding total system cost [35]. So it is essential to select appropriate number of batteries and PV modules to compromise between the system reliability and cost.

In the same matter, Charge controller should be selected carefully depending on the battery voltage level, PV voltage level and the Maximum Power Point (MPP).

4.2 PV Modules

Several types of commercially-available terrestrial modules are available for use in PV systems. The most common PV modules include single- and polycrystalline silicon and amorphous silicon with other technologies (such as copper indium diselenide, cadmium telluride, and hybrid amorphous/single-crystalline silicon modules) entering the market. Modules consist of from a few cells up to dozens of cells interconnected in series and/or parallel as shown in Figure 4.1 to give the desired module voltage and current. The purpose of this section is to give an overview of some of the performance differences between the most common PV module technologies [36].

4.2.1 Crystalline silicon PV modules

Single- and polycrystalline silicon modules as shown in Figure 4.2 have been in use longest and make up more than 80% of the worldwide PV market. Although single-crystalline cells are slightly more efficient than polycrystalline cells, module efficiencies employing either technology are nearly the same. Crystalline- silicon modules have efficiencies ranging from 10 to 15%. High efficiency is an important consideration where array area is limited, for example on the roof of a house or building. Although all module technologies perform better when un-shaded, a small amount of shading (for example from

the branch of a tree or an overhead power line) decreases the output of any module. But typically, crystalline silicon modules are more strongly affected by shading. Crystalline-silicon modules tend to have higher temperature coefficients than amorphous silicon (a-Si): as their temperature increases, their voltage and power output decrease more than for a-Si. Crystalline-silicon modules range in size from the sub-watt level to over 300 W. Larger modules mean fewer to install and fewer interconnects to potentially fail, but special equipment may be required to lift and maneuver larger, heavier modules. Most crystalline-silicon modules contain glass and have rigid frames, making these heavier and more fragile than some other module types [36].

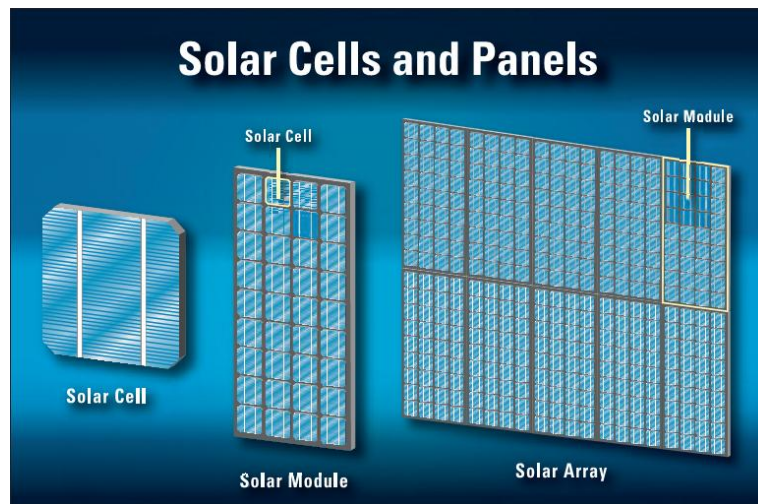


Figure 4.1: Solar Cells and Panels



Figure 4.2: Crystalline silicon PV modules

4.2.2 Amorphous silicon (a-Si) PV modules

Amorphous-silicon modules as shown in Figure 4.3 are one of several types of thin-film technologies. PV manufacturers began manufacturing thin-films to decrease module production costs. Originally, a-Si cells were single-junction devices. With time, manufacturers developed methods of stacking two or three a-Si cells to increase the stabilized module efficiency. Even so, the stabilized efficiency of a-Si modules ranges from about 5% to 7% about half that of crystalline-silicon modules. Lower efficiencies mean that an a-Si array must be larger to achieve the same output as a crystalline-silicon array. Another characteristic the PV system designer must be aware of is the output of a-Si modules drops between 15% and 25% during the first few weeks of exposure to sunlight, after which the output stabilizes to its rated level. Amorphous-silicon modules have some advantages over crystalline-silicon modules. All PV modules perform better under clear skies and at colder temperatures. But at elevated operating temperatures, the output of a-Si modules does not decrease as much as that of crystalline-silicon modules. This can be critical when PV arrays are deployed in hot climates. Typically, at reduced irradiance levels or when partially shaded, the output of a-Si modules decreases less than crystalline silicon modules decrease.



Figure 4.3: Amorphous silicon (a-Si) PV modules

4.2.3 Copper indium diselenide (CIS) PV modules

Copper indium diselenide as shown in Figure 4.4 is a relatively new technology in the PV module market, representing a little more than 0.5% of worldwide sales. Of all the commercially-available thin-film modules, CIS has the highest efficiency at nearly 9.5%. Modules have a flat-black appearance which may make them more aesthetically appealing. This technology presently has a high negative temperature coefficient of voltage and power,

meaning its output will typically decrease more than other module technologies at higher temperatures. Copper indium diselenide modules are available up to 80 W [36].



Figure 4.4: Copper indium diselenide (CIS) PV modules

4.2.4 Cadmium telluride (CdTe) PV modules

Cadmium telluride is a relatively new technology in the PV module market representing a little more than 0.5% of worldwide sales. Cadmium-telluride modules have an efficiency of about 6.5%. They have a flat- black appearance which may make them more aesthetically appealing. The negative temperature coefficient for voltage and power can be comparable or slightly better than that of a-Si (depending on the operating history of the modules), and is generally less than that of crystalline-silicon and CIS. Cadmium-telluride modules are available up to 65 W [36].

4.2.5 Heterojunction with intrinsic thin layer (HIT) PV modules

Heterojunction with intrinsic thin layer or an amorphous-silicon layer on a crystalline-silicon cell, modules have captured more than 5% of worldwide PV sales. By combining both a-Si and crystalline-silicon in a single module, more of the available sunlight is utilized, leading to higher module efficiencies, up to 16%. Presently, the largest HIT module is 190 W [36].

4.3 Batteries

4.3.1 Capacity

The ampere-hour capacity of a battery depends on the size and number of plates of the cells, the amount and concentration of electrolyte (particularly in valve-regulated cells), and the number of parallel strings of cells used. The conditions under which a battery is used can change the available capacity of the battery, as illustrated in the following examples:

- a) Low temperatures reduce capacity
- b) High discharge rates reduce capacity
- c) High end-of-discharge (EOD) voltages reduce capacity
- d) Limitations on the depth of discharge (DOD) reduce capacity
- e) Failure to properly recharge a battery limits its capacity
- f) Excessive periods of high temperature and/or overcharge may result in the loss of water from the electrolyte, premature aging, and limit capacity of batteries

4.3.2 Type

Lead-acid batteries are the most common in PV systems because their initial cost is lower and because they are readily available nearly everywhere in the world. There are many different sizes and designs of lead-acid batteries, but the most important designation is whether they are deep cycle batteries or shallow cycle batteries.

The two generic types of lead-acid batteries are:

- a) Vented: Vented batteries as shown in Figure 4.5 are characterized by plates immersed in liquid electrolyte. The volume of electrolyte is sufficient to allow for a reasonable loss of water by evaporation and by the electrolysis associated with overcharging. A vent in the cell's cover allows a free exchange of the resulting gases with the atmosphere. Catalytic recombiners may be incorporated in each cell vent to reduce water loss. In most of these types of batteries, the lost water can be replaced. [37]



Figure 4.5: Vented Batteries

- b) Valve-regulated: Valve-regulated lead-acid batteries (VRLA) as show in Figure 4.6 are characterized by plates in contact with an immobilized electrolyte. Water loss is minimized during overcharge by oxygen recombination. As long as the cell's recombination rate is not exceeded, the evolved oxygen is recombined at the cell's negative plates to reform water. However, other mechanisms, such as grid corrosion, consume oxygen and lead to water loss and hydrogen evolution. The cell or multi-cell container is sealed with the exception of a pressure-relief valve ("valve-regulated") that allows excess pressure (mostly hydrogen) to be released. In these types of batteries, the lost water generally cannot be replaced. [37]



Figure 4.6: Valve-Regulated Batteries

4.3.3 Cyclability

Lead-acid batteries for PV applications are generally categorized as deep-cycle and shallow-cycle.

4.3.3.1 Deep-cycle batteries

Deep-cycle batteries like the type used as starting batteries in automobiles are designed to supply a large amount of current for a short time and stand mild overcharge without losing electrolyte.

4.3.3.2 Shallow-cycle batteries

Usually, shallow-cycle batteries are discharged less than 25% of their rated capacity on a daily basis Maximum Daily Depth Of Discharge (MDDOD), and up to 80% over the period of autonomy Maximum Depth Of Discharge (MDOD). Manufacturers can supply the maximum number of permissible 80% discharges per year. Typical shallow-cycle-battery PV applications are those with longer autonomy periods.

4.4 Charge Controllers

The main purpose of a charge controller is to prevent the battery from being under- or overcharged. Some additional features of charge controllers may include:

- a) A low-voltage load disconnect to prevent the battery from being over-discharged
- b) Metering or status indicators
- c) Over-current protection
- d) Adjustable settings

4.4.1 Shunt Regulator

Shunt regulators are typically solid-state. Their primary components are a transistor between the array positive and negative lines, and a blocking diode between the battery positive and the array positive. During normal charging, current flows from the array to the battery. When the battery voltage reaches the array disconnect setting, the transistor is activated, shorting the array. The battery is prevented from being shorted by the blocking diode. The blocking diode also prevents the current from flowing back into the PV array from the battery during nighttime. When the battery voltage falls to the array reconnect setting, the transistor is released and the current then flows to the battery again as shown in Figure 4.7.

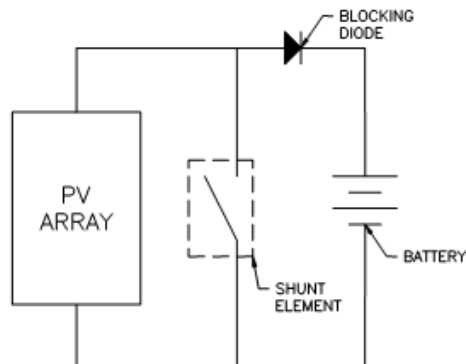


Figure 4.7: Shunt Regulator

This type of charge controller is typically used on smaller low-voltage systems. Although short circuiting the array does not cause damage, there can be large amounts of current flowing through the transistor. The larger the array, the larger the current flowing through the transistor and the larger the amounts of heat the transistor must dissipate. Additionally, voltage drop (loss) occurs across the blocking diode [36].

4.4.2 Series Regulator

Series regulators come in many variations. The basic series regulator consists of a relay (either mechanical or solid-state) between the battery positive conductor and the array

positive conductor (for a negatively grounded system), and a voltage comparator. The negative conductors are used for a positively-grounded system. When the battery voltage reaches the array-disconnect setting, the relay is opened, disconnecting the flow of current to the battery. The PV array becomes open-circuited. When the battery voltage falls to the array-reconnect setting, the relay is closed, allowing the current to flow to the battery again as shown in Figure 4.8 [36].

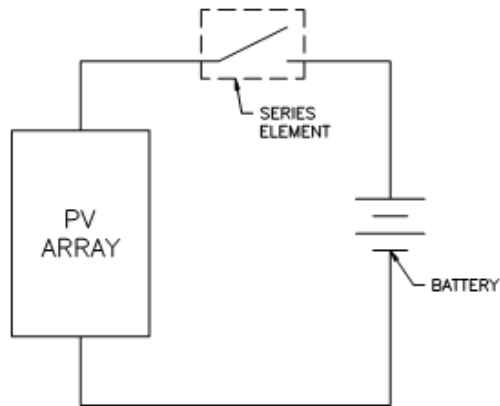


Figure 4.8: Series Regulator

4.4.3 PWM Regulators

A pulse width modulated (PWM) regulator is a variation on the series regulator. The PWM regulator is a series regulator with a solid-state switch instead of a relay. With the solid-state switch replacing the relay, the flow of current from the array to the battery can be switched at high speed (frequencies vary with manufacturers, from a few Hz to kHz). By switching the solid-state switch at high speed, the battery charge voltage can be controlled more accurately. Instead of varying the voltage to control battery charging, the PWM regulator varies the amount of the time the solid-state switch is open or closed by modulating the width of the pulse as shown in Figure 4.9.

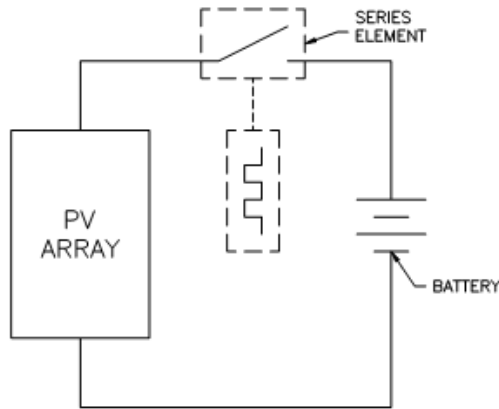


Figure 4.9: PWM Regulator

PWM charge controllers do not require a diode, as the solid-state switch prevents the current from flowing back to the PV array. [36].

4.4.4 MPPT Controllers

The maximum power point tracker (MPPT) charge controller is a variation of the PWM charge controller. The MPPT charge controller as shown in Figure 4.10 adjusts the PWM to allow the PV array voltage to vary from the battery voltage. By varying the array input voltage (while maintaining the battery charge voltage), the maximum output from the PV array can be achieved.

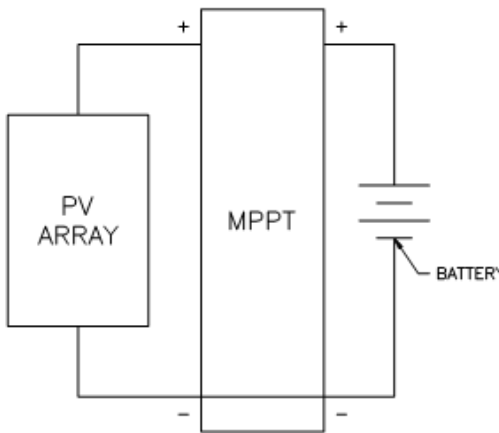


Figure 4.10: MPPT Controllers

The MPPT charge controller is relatively new and has many advantages over other charge regulators. In addition to getting more charge current from the PV array, some MPPT

controllers allow the array to operate at a much higher voltage than the battery. This feature can be useful to reduce wire size and voltage drop from the PV array to the controller. Although the MPPT controller can increase the output from the PV array, they typically have greater losses than the other controller types [36].

4.5 PV & Battery Sizing

In this section, researchers resizing the previous lighting project in Gaza, taking into account the consideration of IEEE Recommendations for Stand-Alone PV Systems in [36] and [37], which are applicable to all stand-alone PV systems where PV is the only charging source as in our case of previous lighting projects.

MATLAB Software is developed in this research for Lighting Projects as a special case, which generating full report of PV and Battery sizing design. Software prompts the user to enter the average load usage, nominal load voltage, autonomy period, maximum load current, and both battery and PV Specifications.

The sequence of procedures to PV and Battery sizing is performed in the following algorithm flowchart and the interface as shown in Figure 4.11, Figure 4.12 respectively.

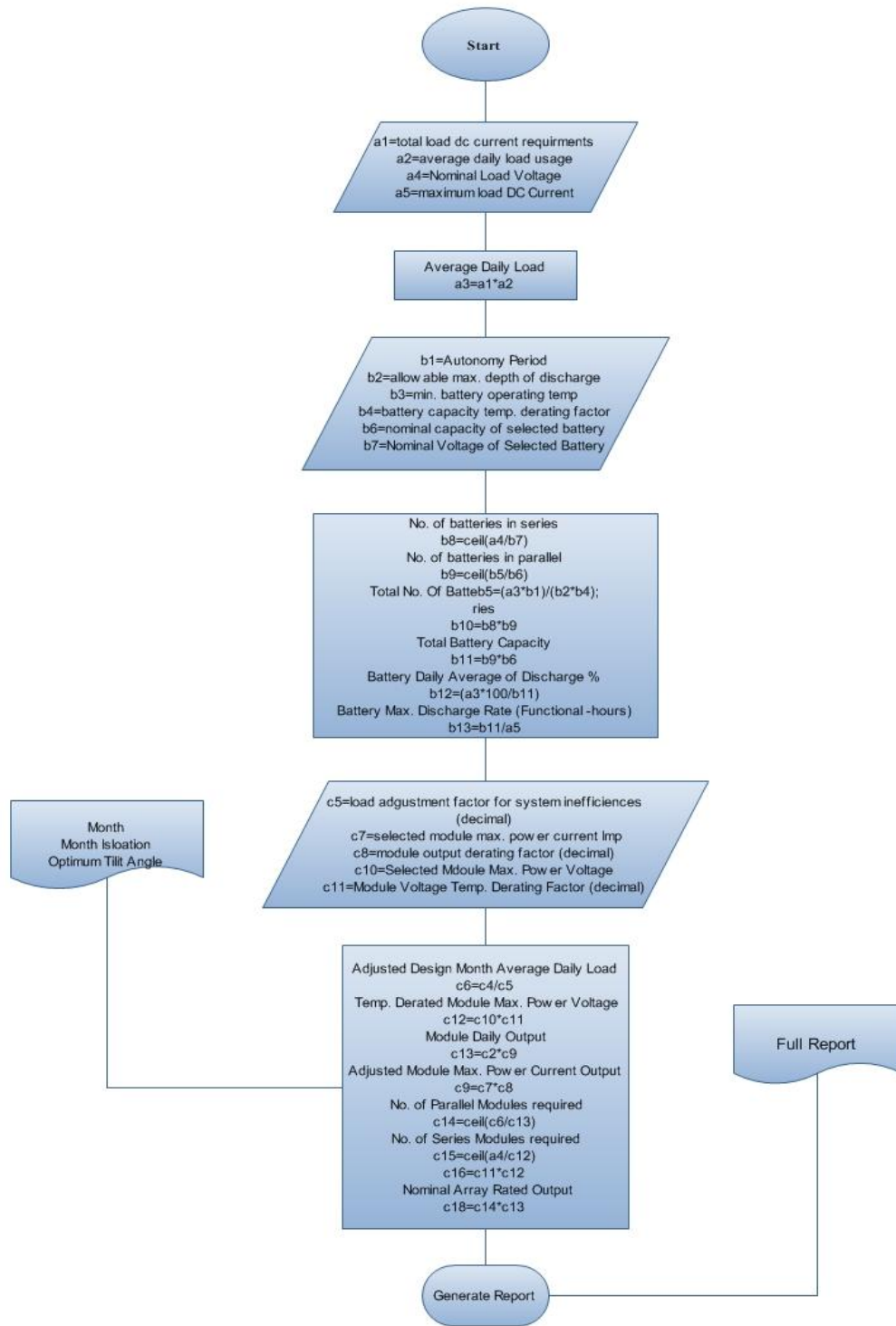


Figure 4.11: PV and Battery sizing software flowchart

The screenshot shows a software interface for PV and battery sizing. It features a grid of input fields with numerical values and a 'Generate Report' button. The parameters and their values are as follows:

Total Load DC current requirements	4.16	Optimal Array Tilt Angle	32
Average Daily Load Usage	4.65	Load Adjustment Factor	0.85
Nominal Load Voltage	12	Imp	5.06
Maximum Load DC Current	4.16	module output derating factor	0.9
Autonomy Period	3	Vmpp	17.8
Allowable Max. Depth of Discharge	0.8	Mod. Voltage Temp. Derating Factor	0.85
Min. Battery Operating Temp	0	Nominal Rated PV Module Output	90
Battery Temp. Derating Factor	0.8		
Nom. Capacity of Selected Battery	100		
Nom. Voltage of Selected Battery	12		
Month	4		
Design Month Insolation	5		

A 'Generate Report' button is located in the lower right quadrant of the interface.

Figure 4.12: PV and Battery sizing software interface

Researchers found several drawbacks in previous design, which degrades the system performance. Table 4.1 shows the difference between the current and the recommended design for PV Lighting Project with the same previously selected batteries and modules.

The major drawbacks in the previous design are the insufficient autonomy period, designing on the maximum month insolation and high percentage of DDOD, while the IEEE recommended settings acquire at least 3 days autonomy period, with designing on the average or minimum month insolation and the percentage of MDDOD should be less than 20% daily.

The proposed redesign for the previous project with different selected batteries and modules is demonstrated in Table 4.1, where the number of batteries is reduced by selecting higher storage capacity, the estimated PV to load ratio is increased which indicates better performance.

Table 4.1: Difference of Sizing Summary between current and recommended designs with same and different selected batteries and modules

<i>Sizing Summary</i>	<i>Current Design</i>	<i>Recommended Design with the same selected Batteries and Modules</i>	<i>Recommended Design with different selected Batteries and Modules</i>
<i>Lighting Load (Ah/13hrs.day)</i>	39	39	39
<i>Average Month Insolation(kWh/m2/day)</i>	7	5	5
<i>Design Autonomy Period (days)</i>	< 1	3	3
<i>Selected Battery (S×P)</i>	1×2	1×4	1×2
<i>Total No. of Selected Batteries(#)</i>	2	4	2
<i>Battery Storage Capacity (Ah)</i>	60	60	150
<i>Allowable Depth of Discharge Limit (%)</i>	No Limit	80	80
<i>Average Daily Depth of Discharge DDOD (%)</i>	32.5	16.2500	13
<i>Selectd Module (S×P)</i>	1×1	1×2	1×2
<i>Total No. of Selected Modules(#)</i>	1	2	2
<i>Nominal Rated PV Module Output (watt)</i>	135	135	135
<i>Estimated PV to Load Ah Ratio</i>	1.3462	1.9231	1.9564

4.6 Discussion and Conclusion

Frankly, the previous project is not designed carefully, designers didn't take into their account the IEEE Recommendation for PV and Battery sizing, which maintains the lifetime of solar system. Table 4.1 shows the difference between several designs, where the performance is measured depending on the value of estimated PV to Load ratio.

The recommended design done using the developed MATLAB Software meets the system requirements and IEEE recommendations with duplication of batteries and PV modules.

The developed MATLAB Software is very useful to PV designers and consultants in Authority of Energy in Palestine, which simplifies the PV and Battery sizing calculations, taking into account the IEEE Recommendations and global solar radiation of Palestinian Territories.

The software will be developed later to provide more options for BIPV designers and consultants, also to generate web-based PDF report.

Chapter 5

Experimental Model: Stand-Alone Photovoltaic System for Home Lighting

5.1 Introduction

This chapter covers an experimental solar model for home lighting. This model has been developed to be alternate solution for the drop of Grid electricity due to the Siege, shortage of fuel supplies, and maintenance problems.

The designed solar model should meet the lighting load for an apartment of $180m^2$, it consists of 2 bed rooms, 3 living rooms, kitchen and bathroom. The experimental model as shown in Figure 5.1 consists of 85 peak-watts PV module, a 100Ah lead-acid storage battery, a 12V DC boost solar charge regulator, and 12V DC/220V AC Inverter.

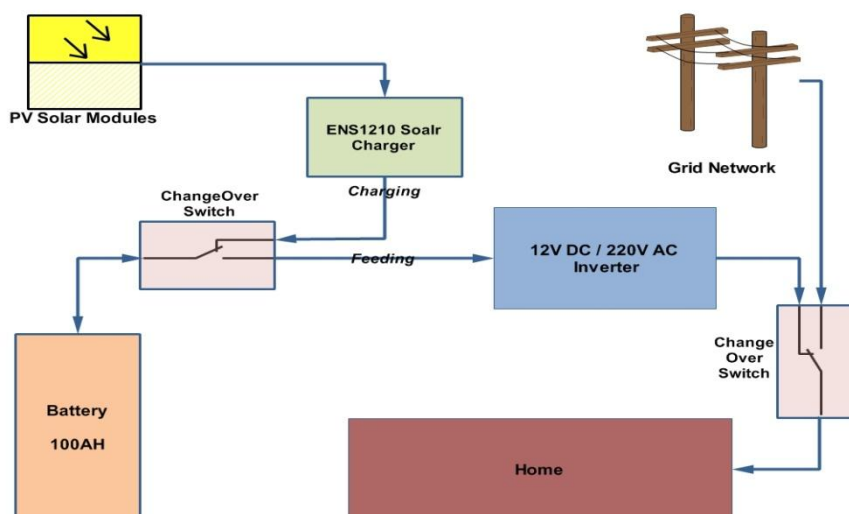


Figure 5.1: Schematic Diagram of Experimental Solar Model

5.2 System Design and Implementation

Based on the results obtained in this research, the following section presents the control system design and implementation as follows:

5.2.1 Orientation and Tilt angle

According to the elevation view map of the desired location in Figure 5.2, the home is located 45° west to the true south, so the PV module should be located 180° facing to the south, with different seasonal tilt angle as described previously.



Figure 5.2: Elevation View of Home from Google Earth®

5.2.2 Calculating Load Consumption

Since the Project for lighting an apartment, so the load consumption table is not difficult, while if it is used for powering the apartment, the load consumption will be different.

In this experiment, both scenarios; lighting and powering the apartment will be described here, with focusing on lighting the apartment. Electrical load could be classified as follows:

5.2.2.1 Momentary current

Loads lasting 1 min or less are designated “momentary” loads and are given special consideration. The ampere-hour requirements of this type of load are usually very low, but

their effect on battery terminal voltage may be considerable and should be taken into account. Momentary loads can occur repeatedly during the duty cycle. Typical momentary loads are:

- a) Motor starting currents
- b) High inverter surge currents

5.2.2.2 Running current

Running current is the current required by a load after its starting current has subsided. Certain devices require a constant power, thus the required current rises as the battery voltage falls.

Typically, Table 5.1 described the average daily load for the apartment either for powering or lighting purpose.

Table 5.1 : Apartment Electrical Load

<i>Electrical Load</i>	<i>Wattage (Watt)</i>	<i>Average Time Duration (hrs)</i>	<i>Powering (Watt)</i>	<i>Lighting (Watt)</i>
<i>Lighting(5 units-3 as average)</i>	<i>3×15</i>	<i>3/5</i>	<i>135</i>	<i>225</i>
<i>Wireless Telephone</i>	<i>7</i>	<i>3</i>	<i>21</i>	<i>-</i>
<i>DVD Player</i>	<i>18</i>	<i>3</i>	<i>54</i>	<i>-</i>
<i>DVB Digital Receiver</i>	<i>35</i>	<i>3</i>	<i>105</i>	<i>-</i>
<i>Television</i>	<i>85</i>	<i>3</i>	<i>255</i>	<i>-</i>
<i>Laptop(2 units)</i>	<i>2×80</i>	<i>3</i>	<i>480</i>	<i>-</i>
<i>ADSL Router</i>	<i>15</i>	<i>3</i>	<i>45</i>	<i>-</i>
<i>Total Load</i>			<i>1095</i>	<i>225</i>

In order to obtain the required data for MATLAB software, Average daily DC current should be computed as follows:

$$\text{DC/AC Inverter efficiency equals } (\eta_{inv}) = \frac{P_{out}}{P_{in}} = \frac{P_{AC \text{ Load}}}{P_{DC \text{ Load}}} \approx 90\%$$

$$\text{Average Daily DC Current } (I_{Avg}) = \frac{P_{DC \text{ Load}}}{\text{Battery Voltage}} = \frac{P_{AC \text{ Load}}}{\eta_{inv} \times \text{Battery Voltage}}$$

5.2.3 PV Components

The PV module is mounted on the roof of building as shown in Figure 5.3, the available PV module (Appendix A.1) in Gaza Strip was 90 Wp, which has maximum voltage (Vmp) of 17.8 V, while the maximum output current (Imp) of 5.02 A.



Figure 5.3: Mounted PV Module on roof building

The Battery used in this experiment is Lead Acid Battery of 100 AH, where the boost PWM controller used here to adapt the PV module voltage to the battery voltage of 12V DC, it is very important to include it in the solar power system to reduce battery replacement, the selected controller (Appendix A.2) as shown in Figure 5.4 regulates the charging process of 12V DC Battery, with short circuit and overload protection.

Unfortunately, the available one is rated to 10A, which implies that the maximum load power is 120W. In order to overcome this problem, changeover switch as shown in Figure 5.5 is used here to bypass the solar charge controller to provide the required current without facing overloading problem; the changeover switch is designed to maximum drawn current of 50A.



Figure 5.4: ENS1210 Solar charge Controller



Figure 5.5: ENS1210 Solar charge controller with changeover switch

The DC/AC Inverter (Appendix A.3) is used here in this experiment to handle AC loads in the apartment, the available inverter in Gaza strip is between (350 – 1000)W, the selected one for this project is 500W as shown in Figure 5.6, changeover switch is used here again for switching between grid network and solar system with light indicators.



Figure 5.6: 500W Inverter with changeover switch between grid network and solar system

5.3 Results and Discussion

5.3.1 PV and Battery Sizing

Table 5.2 shows the Battery and PV sizing for the experimental model, taking into account the IEEE recommendations [36] and [37]. Unfortunately, the PV modules, Voltage Regulators and inverters, which are available in Gaza strip, are limited. So the system design is done backwardly, depending on the available PV modules and other components. The experiment covers an apartment with the previous load described in Table 5.1 for five hours lighting and half hour for powering taking into account the IEEE Recommendations.

While the proposed design for powering the apartment for six hours could be summarized in Table 5.3, the proposed design could not be implemented because of hardware and components limitations.

PV and Battery Sizing is considered one of the most important steps in designing solar model, because its direct effect on cost, which is the main role in the design process.

Table 5.2: Sizing Summary for an Apartment

<i>Sizing Summary</i>	<i>Lighting ≈5hrs</i>	<i>Powering 0.5hrs</i>
<i>Average DC Current Load (Ah/day)</i>	4.16	33.8
<i>Average Month Insolation(kWh/m2/day)</i>	5	5
<i>Design Autonomy Period (days)</i>	3	1
<i>Selected Battery (S×P)</i>	1×1	1×1
<i>Total No. of Selected Batteries(#)</i>	1	1
<i>Battery Storage Capacity (Ah)</i>	100	100
<i>Allowable Depth of Discharge Limit (%)</i>	80	80
<i>Average Daily Depth of Discharge DDOD (%)</i>	19.344	16.9
<i>Selectd Module (S×P)</i>	1×1	1×1
<i>Total No. of Selected Modules(#)</i>	1	1
<i>Nominal Rated PV Module Output (watt)</i>	90	90
<i>Estimated PV to Load Ah Ratio</i>	1.3079	1.4852

Table 5.3: Sizing Summary for proposed model

<i>Sizing Summary</i>	<i>Case I</i>	<i>Case II</i>
<i>Average DC Current Load (Ah/day)</i>	33.8	16.9
<i>Average Month Insolation(kWh/m2/day)</i>	5	5
<i>Design Autonomy Period (days)</i>	3	3
<i>Battery Volatge (Volts DC)</i>	12	24
<i>Selected Battery (S×P)</i>	1×10	1×3
<i>Total No. of Selected Batteries(#)</i>	10	3
<i>Battery Storage Capacity (Ah)</i>	100	200
<i>Allowable Depth of Discharge Limit (%)</i>	80	80
<i>Average Daily Depth of Discharge DDOD (%)</i>	20.28	16.9
<i>Selectd Module (S×P)</i>	1×11	1×4
<i>Max. Module Voltage (Vmpp)</i>	17.8	32.3
<i>Max. Module Current (Impp)</i>	5.06	7.75
<i>Total No. of Selected Modules(#)</i>	11	4
<i>Nominal Rated PV Module Output (watt)</i>	90	210
<i>Estimated PV to Load Ah Ratio</i>	1.3614	1.5286

5.3.2 Cost Estimation

It varies. Depending on the PV and battery sizing, the amount of required electricity, the particular solar energy system, how much sunshine received in our area. Table 5.4 shows the comparison between the available energy sources in Gaza Strip, Palestine, and the cost estimation per kilo watt hour (\$/KWhr).

Unfortunately, price of solar system components is very expensive compared to those outside Gaza Strip, Palestine, which increases the cost of solar energy, another factor is the

availability of solar components, which restricts the designer to particular components that increases the cost of solar system.

Here are the outlined equations for cost estimation:

$$\text{Cost}(\$/K\text{Whr}) = \frac{\text{Total Cost over 20 years}}{\text{Total Load for 20 years}}$$

$$\begin{aligned} \text{Total Cost for 20 years} \\ &= \text{Installation Cost} + \text{Accumulative Running Cost for 20 years} \\ &+ 20 \text{ Years} * (\text{Maintenance Cost} + \text{Parts Replacement}) \end{aligned}$$

$$\begin{aligned} \text{Accumulative Running Cost for 20 years} \\ &= (\text{Total Yearly Load} * \text{Yearly Running Cost}) + \text{Previous Years Cost} \end{aligned}$$

$$\begin{aligned} \text{Yearly Running Cost} \\ &= \text{Previous Year Running Cost} * (1 + \text{Incremental Cost Percentage}) \end{aligned}$$

Table 5.4: Comparison for cost estimation between available source energy for home user

<i>Items</i>	<i>Solar Energy</i>	<i>Grid Network</i>	<i>Diesel Generator</i>
<i>Average Daily Load/Day (KWhr)</i>	<i>1 KWhr</i>	<i>1 KWhr</i>	<i>1 KWhr</i>
<i>Total Yearly Load (KWhr/year)</i>	<i>360</i>	<i>360</i>	<i>360</i>
<i>Expected Lifetime (years)</i>	<i>20</i>	<i>100</i>	<i>3</i>
<i>Total Load for Expected PV Lifetime (KWhr)</i>	<i>7200</i>	<i>7200</i>	<i>7200</i>
<i>Installation Cost (\$)</i>	<i>1040</i>	<i>300</i>	<i>150</i>
<i>Running Cost (\$/KWhr)</i>	<i>-</i>	<i>0.17</i>	<i>0.5</i>
<i>Incremental Cost Percentage (%\$/Year)</i>	<i>-</i>	<i>0.01</i>	<i>0.01</i>
<i>Yearly Maintenance (\$/Year)</i>	<i>-</i>	<i>-</i>	<i>30</i>
<i>Parts Replacements (\$/Year)</i>	<i>35</i>	<i>-</i>	<i>53</i>
<i>Cost/KWhr</i>	<i>0.28</i>	<i>0.23</i>	<i>0.81</i>

5.3.3 Conclusion

Unfortunately, price of solar system components is very expensive compared to those outside Gaza Strip, Palestine, which increases the cost of solar energy, another factor is the availability of solar components, which restricts the designer to particular components that increases the cost of solar system.

Chapter 6

Conclusions and Recommendations

6.1 Introduction

In this research, a solar system model designed with consideration of IEEE standards and recommendations is presented here. This model has been developed after studying previous projects implemented in Gaza strip, and handles the drawbacks in these projects.

The Re-Design and Re-Evaluation process for lighting and controlling projects in Gaza Strip expands and motivates the researcher to provide solutions for the current situation, and directing this great interest to this field.

6.2 Conclusion

The following points reflect the major contributions to the research:

1. Developing Empirical Model to estimate the global solar radiation for Gaza Strip, Palestine is considered the first contribution of this research which helps the designer and engineers to estimate the intercepted solar radiation which is a first step towards any successful design for solar project. The developed model used Angstrom equations; both linear and polynomial model, the estimated model is similar to the observed data with good agreement.
2. Both optimum tilt and azimuth angles for PV module were derived using mathematical equations in this research, the optimum azimuth angle is found 180° facing to south, while the optimum tilt angle is found as the geographical latitude of Gaza Strip 31.464° .
3. Novel design of one axis two position manual tracking PV module was proposed and considered as a second contribution, the results show that the power generation of the novel design can be increased by 17%, 3% of the previous design and the optimum design respectively without any additional cost. The manual orientation should be done twice a year as a maintenance task.
4. Researcher focuses on the PV and Battery sizing which was main drawback in the previous design, the recommended design is proposed using the developed MATLAB Software meets the system requirements and IEEE recommendations of Sizing process. The developed MATLAB Software is considered as a third

contribution of this research, which helps PV designers and consultants in Authority of Energy in Palestine to make calculations for the PV and Battery sizing process, taking into account the IEEE Recommendations and global solar radiation of Palestinian Territories.

6.3 Recommendations and Future Work

- The issue of uncertainty to component variation by aging or environment needs to be studied in details to provide a robust control for such systems.
- Actually, it has become necessary to make the best efforts to increase renewable energy projects especially in this decade, where other countries such as Germany has a rapid growth in this technology in the previous decade by 95% [38]. It is recommended to support stand-alone individual projects for home and clinics to overcome the shortage in electricity.
- On the other side, decision and policy makers should take decisive measures to support development and energy programs especially after the Israeli siege on Gaza Strip.
- Finally, it is really hoped that this research can be used as guidance and a pilot program for future solar projects in Palestine.

References

- [1] UNDP. “World Energy Assessment”, United Nations Development Programme , NewYork , 2009, 92-1-126126-0, 2009.
- [2] Yaseen, Basel T. Q. “Renewable Energy Applications in Palestine”, Palestinian Energy and Environment Research Center (PEC)- Energy Authority, Palestine, 2007.
- [3] Widén, Joakim. “Distributed Photovoltaic in the swedich energy systems”. The Faculty of Science and Technology, Uppsala University , Uppsala, Sweden, 2009.
- [4] M.S. Alam et al. “Simulation of Solar Radiation System,” *American Journal of Applied Science*, Science Publication, Vol. 2, 2005.
- [5] Danny H.W.Li and Tony N.T. Lam. “Determining the Optimum Tilt Angle and Orientation for Solar energy Collection Based on Measured Solar Radiance Data,” *International Journal of Photoenergy*, Hong Kong , 2007.
- [6] Jurgita Grigonienė, Mindaugas Karnauskas. “Mathematical modeling of optimal tilt angles of solar collector and sunray reflector,” *Energetika*, Lithuania, 2009.
- [7] D.FAIMAN and D.R.MILLS. “Orientation Of Stationary Axial Collectors,” *Solar energy*, Sydney, Australia, 1992. 0038-092X/92.
- [8] Calabrò, Emanuele. “Determining optimum tilt angles of photovoltaic panels at typical north-tropical latitude,” *Journal of Renewable and Sustainable Energy Messina*, Italy, 2009. 033104/6.
- [9] Huan-Liang Tsai, Ci-Siang Tu, and Yi-Jie Su. “Development of Generalized Photovoltaic Model Using MATLAB/SIMULINK,” *Proceeding of the World Congress on Engineering and Computer Science*, San Frasesco, USA, 2008. 978-988-98671-0-2.
- [10] Cristian Dragoş Dumitru, Adrian Gligor, “Software Development for Analysis of Solar-Wind Hybrid Systems Supplying Local Distribution Networks,” *2nd International Conference on Modern Power Systems MPS 2008*. CLUJ-NAPOCA, ROMANIA, 2008.
- [11] *A Novel Modeling Method for Photovoltaic Cells* . Aachen, Germany : 35th Annual IEEE Power Electronics Specialists Conference , 2004. 7803-8399.

- [12] Weidong Xiao, William G. Dunford, Antoine Capel, Trishan Eram, Patrick L. Chapman. "Comparison of Photovoltaic Array Maximum Power Point Tracking Techniques," *IEEE Transaction on Energy Conversion*. 2007, Vol. 22, 2.
- [13] Tamer Khatib, Azah Mohamed, Nowshad Amin. "A New Controller Scheme for Phtovoltaic Power Generation Systems," *European Journal of Scientific Research Selangor, Malaysia*, 2009, Vol. 33.
- [14] Aretaga Orozco, J.R. Vazquez, P.Saleron, S.P. Litran, F.J. Alcantara. "Maximum power point tracker of a photovoltaic system using sliding mode control". 2009.
- [15] il-Song Kim, Pyeong-Sik Ji, Un-Dong Han, Chin-Gook Lhee, Hong-Gyu Kim. "State Estimator Design for Solar Battery Charger," *Chung-Ju National University, Republic of KOREA, IEEE*, 2009.
- [16] Supartim Basu, Lars Norum, Dhaval Dalal. "An Improved PV Battery Charger for Low Cost Low Power Stand Alone Low Power Systems," *ICSET 2008*, 2008. 4244-1888.
- [17] Weidong Xiao, Willaim Dunford. Topology Study of Photovoltaic Interface for Maximum Power Point Tracking. *IEEE Transaction on Industrial Electronics*. 2007, Vol. 54, 3.
- [18] Hussein, Mohammed Tawfik. "A Novel Algorithm to Compute All Vertex-Matrices of an Interval Matrix: A Computational Approach," *International Journal of Computing & Information Sciences*, 2004, Vol. 2.
- [19] A.Naim, O.Al-Najjar, A.Kassem. *Project Research, Building Electrification Using Phtovoltaic System*. Gaza : Ministry of Energy and Natural Resources, 2003.
- [20] Gaza Strip. *wikipedia*. [Online] 18 December 2009 . [Cited: 19 December 2009.] http://en.wikipedia.org/wiki/Gaza_Strip.
- [21] CIA-The WorldFact- Gaza Strip. *CIA*. [Online] 3 November 2009. [Cited: 19 December 2009.] <https://www.cia.gov/library/publications/the-world-factbook/geos/gz.html>. 1553-8133.
- [22] Ridha Fethi Mechlouch and Ammar Ben Brahim. "A Global Solar Radiation Model for the Design of Solar Energy Systems," *Asian Journal of Scientific Research, Gabes, Tunisie*, 2008, Vol. 1. 1992-1454.

- [23] B. Safari and J. Gasore. "Estimation of Global Solar Radiation in Rwanda Using Empirical Models," *Asian Journal of Scientific Research*, Huye, Rwanda, 2009, Vol. 2. 1992-1454.
- [24] Firoz Ahmad, Intkhab Ulfat. "Empirical Models for the correlation of Monthly Average Daily Global Solar Radiation with Hours of Sunshine on a Horizontal Surface at Karachi, Pakistan. Karachi", *Turk J Phys*, Pakistan, 2004, Vol. 28.
- [25] Ahmed, Mohammed Rabia, "Potential of Application of PV System for BWRO Desalination in Gaza," *GCREEDER 2009*, Amman, Jordan, 2009.
- [26] *Renewable And Conventional Energy Technology*.
- [27] COOPER, P. I. "Digital simulation of transient solar still process," *Solar Energy*, 1969, Vol. 12.
- [28] Gaza, Meteorological Station in. *Model for Global Solar Radiation using Gaza and Bet Dagan Stations*. Gaza : s.n.
- [29] 585A, GEOS. *Lecture Notes_11*. Spring 2009.
- [30] Hongxing Yang, Lin Lu. Hong Kong. "The Optimum Tilt angle and Orientations of PV Claddings for Building -Integrated Photovoltaic (BIPV) Applications," *Journal of Solar Energy Engineering*, 2007.
- [31] Chang, Tian Pau. "Study on the Optimal Tilt Angle of Solar Collector According to Different Radiation Types," *International Journal of Applied Science and Engineering*, Nantou 542, Taiwan, 2008. 1727-2394.
- [32] Hanieh, Ahmed Abu. "Automatic Orientation of Solar Photovoltaic Panels," *GCREEDER 2009*. Amman, Jordan, 2009.
- [33] B.J. Huang and F.S. Sun. "Feasibility study of one axis three positions tracking solar PV with low concentration ratio reflector" *Science Direct*, Taipei 106i, Taiwan :, 2006. 0196-8904.
- [34] Mohammed Hussein, Shadi Albarqouni. "Developing Empirical Models for Estimating Global Solar Radiation in Gaza Strip, Palestine". *Journal of The Islamic University of Gaza*, Gaza, Palestine, 2010.
- [35] BELFKIRA, HAJJI, NICHITA and BARAKAT. "Optimal Sizing of stand-alone hybrid wind/PV system with battery storage," 76058 Le Havre, France, 2008.

- [36] *IEEE Recommended Practice for Sizing Lead-Acid Batteries for Stand-Alone Photovoltaic (PV) Systems*, IEEE, 2007. IEEE std 1013-2007.
- [37] *IEEE Guide for Array and Battery Sizing in Stand-Alone Photovoltaic Systems.*: IEEE, 2008. IEEE Std 1562-2007.
- [38] *Renewable Energy World Magazine*(13)1, 2010, 40-45.

Appendix A

Technical Specifications

A.1 PV Modules

carSPA | **ENpower** Solar Modules ESM-085
WENZHOU CARSPA ELECTRONICS TECHNOLOGY CO.,LTD.

125 Monocrystalline 85Wp (ESM-085)

Electrical Characteristics			
Module No.	ESM-085		
Pmax(Wp)	90Wp	85Wp	80Wp
Isc(A)	5.45	5.21	4.98
Voc(V)	22.4	22.3	22.3
Vmax(V)	17.8	17.7	17.6
Imp(A)	5.06	4.8	4.55
Tolerance(W)	±2.5W		
Cell Matrix	9x4		
Max.system Voltage Vmax	DC1000V		
Noct	47±2°C		
Power tem.coeff.(/°C)	- (0.4±0.05) %		
Current temp.coeff. (/°C)	(0.065±0.015) %		
Voltage temp.coeff. (/°C)	- 0.38%		
Ambient temperature (°C)	- 40~85		
Max.mechanical load	245kg/m ²		
Test condition	1000W/m ² ,AM1.5,25°C±2°C		
Dimension Characteristics			
Length	1178mm		
Width	994mm		
Height	45mm		
Weight	14.5mm		
Cell type	mono-crystalline Si (156mm×156mm)		
Cell number	42 pcs		
<p>frame cross view</p> <p>Note: These characteristics are applicable to all types of modules in this catalogue. Please contact us if you have any other needs.</p>			

A.2 Solar Charge Controller

carSPA | ENpower Solar charger controller ENS Series WENZHOU CARSPA ELECTRONICS TECHNOLOGY CO.,LTD.

■ BENEFITS OF THE SOLAR CONTROLLER

It is very important to include a controller in a solar power system.

- 1.Reduce the cost of battery replacements
- 2.Provides useful information

■ ADVANTAGES OF THE ENS Series CONTROLLER

- 1.Low Cost
- 2.High Reliability
- 3.Electronic Protections
- 4.Easy to Use

■ Main Characters:

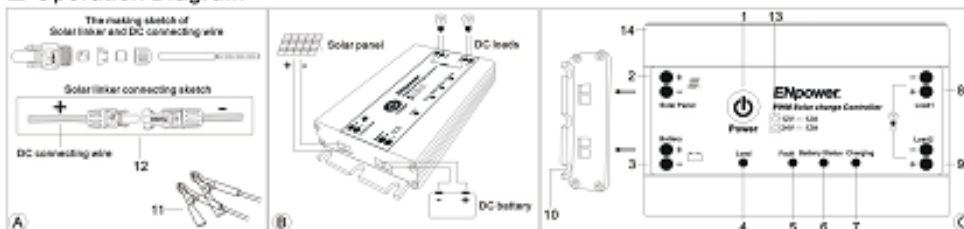
- 1.Microcontroller Digital Accuracy
- 2.OWM charging Mode
- 3.Temperature Compensation; with External Temperature Sensor
- 4.Fully Automatic Operation & Electronic Protection
- 5.Digital LED Display

■ Specification

Order NO.	ENS1206	ENS1210	ENS1212	ENS1216
Rated Solar Input	5A	10A	12A	15A
Rated Load	5A	10A	12A	15A
System Voltage	12V			
Short Circuit and Over Load Protection	Yes			
Self-Consumption	≤ 6mA			
Low Voltage Reconnect	≤ 0.26V			
Low Voltage Disconnect	≤ 0.15V			
Over Voltage Protection	17V			
Using Temperature	-35℃ ~ +55℃			
Boost Voltage(10 Minutes)	14.4V			
Equalization Voltage(10 Minutes)	14.4V			
Floating voltage	13.6V			
Charging Return Voltage	13.2V			
Low Voltage	11.1V			
Over Discharge Voltage	11.1-self-consumption voltage			
Over Discharge Return Voltage	13.0V			
Control Way	PWM			
Packing Details				
Size	122*68*20mm(L*W*H)			
Weight	250g			
Inner Box	Quantity:10pcs			
	Dimension:28.5*27.5*17.5cm			
Carton	Dimension:56*30*36.5cm			
	N.W:10kg G.W:12kg			



■ Operation Diagram



■ The Instruction of Controllers

- | | | | | |
|--------------------------|----------------------|-----------------|---|--------------------------------|
| 1.Button | 4. Load LED | 7. Charging LED | 10. Installation Hole | 13. Rated Voltage Current Data |
| 2. Solar Panel Connector | 5. Fault LED | 8. Load 1 | 11. Battery Clip | 14. Aluminum Alloy Shell |
| 3. Battery Connector | 6. Battery state LED | 9. Load 2 | 12. Solar Linker(it need to be choosed by yourself) | |

A.3 DC/AC Inverter



Inverter Expert *CarSPA*
CAR series CAR500U-500W

Features:

- 12V or 24V DC input
- Power ON-OFF switch
- Input voltage range: -15%~+25%
- Output voltage regulation: ±10%
- Protections: Bat. Low alarm/Bat. Low shutdown/Over voltage/Over temp./Output short/ input polarity reverse/Over load.
- Output waveform: Modified sine wave
- Auto built-in Cooling fan
- Topology: Microprocessor
- Light weight and slim
- AC outlets: Optional
- Approvals: CE / RoHS
- 1.5 year warranty

500W RATED POWER
1000W SURGE POWER
1.5 YEAR LIMITED WARRANTY

AC Output Receptacles (optional)



Specification:

DRIVER No. (With Universal Web USB Output Port)	CAR500U-121	CAR500-121	CAR500U-122	CAR500-122	CAR500U-241	CAR500-241	CAR500U-242	CAR500-242
AC VOLTAGE	100/110/120VAC		220/230/240VAC		100/110/120VAC		220/230/240VAC	
RATED POWER	500W							
SURGE POWER	1000W							
USB	5V/500mA (Without USB, Model No.: CAR500-***)							
WAVEFORM	Modified Sine Wave							
FREQUENCY	50Hz ± 5.00Hz ± 3							
AC REGULATION	± 10%							
STANDARD RECEPTACLES	A, B, C, D, E, F, G, H, I, J, K, L, M, N, O, P, Q, R, S, T, U, V, W, X, Y, Z							
LED INDICATOR	Green LED for power on, Red LED for power failure status							
DC CURRENT	50A							
NO-LOAD CURRENT DRAW	< 0.8A							
DC VOLTAGE	12V							
VOLTAGE RANGE	10~15VDC							
EFFICIENCY (Typ.)	> 90%							
DC CONNECTOR	Battery clip/15A Battery cord 550mm 5VR6*20A							
FUSE(BUILT-IN)	30A*20A							
AC OVERLOAD POWER	10.8 ± 0.6V							
BAT. LOW ALARM	10 ± 0.5V							
BAT. LOW SHUTDOWN	11.5-12V							
BAT. LOW VOLTAGE RECOVER	15.5 ± 0.5V							
OVER VOLTAGE	550W-650W							
OVER TEMPERATURE	45 ± 5°C / 113 ± 9°F							
SHORT CIRCUIT	Shut-off							
BAT. POLARITY	By fuse open							
WORKING TEMP.	0-30°C @ 100% load 40°C @ 50% load							
WORKING HUMIDITY	20%-90% RH non-condensing							
STORAGE TEMP./HUMIDITY	-30~+70°C / -22~+158°F 10-95% RH							
TEMP. COEFFICIENT	± 0.05%/°C (0-50°C)							
UNIT SIZE	238*102*55.5mm(L*W*H)							
WEIGHT(G)	1250g							
MEASURE(V/C/T)	50/30/45cm							
N.W/G.W.	18.7kg/27.5kg							
QUANTITY(C)	20pcs							





File Name: CAR500-spec_2009-12-04

Appendix B

MATLAB Code

B.1 Angstrom's Equation Code

```
Lhy=[ 6 7 7.5 9 10.5 12 12 11.5 10 9 7 6 ];
months=[31 28 31 30 31 30 31 31 30 31 30 31];
ny =[15 46 74 105 135 166 196 227 258 288 319 349];
Hg1=[2.6081 3.3971 4.6972 5.8639 6.8834 7.5528 7.2916 6.6666 5.6944 4.2529 3.0944 2.475]; %reference
to Bet Dagan (1991-2005)
Hg2=[3.24 4.01 5.32 6.34 7.20 7.65 7.80 7.16 6.29 4.94 3.89 3.03]; % reference to Location using
METEONORM 6.1.0.17
Hg3=[3.36 3.97 4.33 5.19 6.46 7.78 7.40 6.76 5.88 4.73 4.31 3.53]; % reference to Besor Farm (1993-2002)

Lm=[];
wsr=[];
wsd=[];
Ho=[];
How=[];

for i=1:12
%=====
Lhy(i); % Monthly Average Solar Day Length in Hours
% =====
% Calculating the Sunshine hour Angle, Maximum Length Day
% =====
phi=deg2rad(31.464); % Latitude Degree 31.464
delta=deg2rad(23.45*(((sin(deg2rad((360/365)*(284 + ny(i))))))))); % Declination Angle
wsr(i)=acos(-tan(phi)*tan(delta));
wsd(i)=rad2deg(wsr(i));
Lm(i)=(2/15)*wsd(i);
% =====
% Calculating the Daily Global Radiation on a m2 horizontal Surface at the location on
% clear sky day in the month Ho
%=====
Isc=1.367e3*3600;
Ho(i)=
(24/pi)*Isc*(1+0.033*cos(deg2rad(360*ny(i)/365)))*(wsr(i)*sin(phi)*sin(delta)+cos(phi)*cos(delta)*sin(wsr(
i)));
How(i)=Ho(i)/3600000; % Ho in kWhr/m2.day
%=====
end

L=Lhy./Lm;
H1=Hg1./How;
H2=Hg2./How;
H3=Hg3./How;
% Havg=(H1+H2+H3)/3;
```



```

Havg=(H1+H2)/2;

% a=-0.002351;
% b=0.7607;
% after modification on phi angle
a=0.2447;
b=0.4871;

Hg=(a+(b*L)).*How;

% e=-0.7551;
% d=1.868;
% c=-0.3941;
%after modification on phi angle
e=-1.183;
d=2.234;
c=-0.3864;
Hgm=(c+(d*L)+(e*L.^2)).*How;

plot(1:12,Hg)
hold on
plot(1:12,Hgm,'r')
grid on
legend('1st Order Model', '2nd Order Model')
xlabel('months')
ylabel('Solar insolation kWhr/m2')

```

B.2 Optimum Angle

```

close all;
phi=deg2rad(31.464);
zetaa=180;
y=[];
optindexa=[];
Ho=[];
Ht=[];
Htm=[];

for betaa=0:60;

    for n=1:365;
        % =====
        % Calculating the Sunchine hour Angle, Maximum Length Day
        % =====
        delta=deg2rad(23.45*(((sin(deg2rad((360/365)*(284 + n)))))));
        beta=deg2rad(betaa);
        zeta=deg2rad(zetaa);
        wsr=acos(-tan(phi)*tan(delta));
        y(betaa+1,n)=(sin(phi)*(sin(delta)*cos(beta)+cos(delta)*cos(zeta)*(cos(wsr)*sin(beta)))+
        cos(phi)*(cos(delta)*cos(wsr)*cos(beta)-
        sin(delta)*cos(zeta)*sin(beta))+cos(delta)*sin(zeta)*sin(wsr)*sin(beta));
        % =====
        % Calculating the Daily Global Radiation on a m2 horizontal Surface at the location on
    end
end

```

```

% clear sky day in the month Ho
% =====
Isc=1.367;
Ho(betaa+1,n)=
(24/pi)*Isc*(1+0.033*cos(deg2rad(360*n/365)))*(wsr*sin(phi)*sin(delta)+cos(phi)*cos(delta)*sin(wsr));
Ht(betaa+1,n)=Ho(betaa+1,n).*y(betaa+1,n);
end

Htm(betaa+1)=mean(Ht(betaa+1,:));
Htmax=max(Htm);
plot(1:365,Ht(betaa+1,:))
hold on

% optang(betaa+1)=max(Ht(betaa+1,:));
% optindex=[betaa optang(betaa+1)];
% optindexa=[optindexa ; optindex];
end

```

B.3 PV Sizing

% PV Lighting System Sizing Worksheet

```
function [o1,o2,o3,o4,o5,o6,o7,o8]=pv_sizing(a1,a2,a4,a5,b1,b2,b3,b4,b6,b7,c1,c2,c3,c5,c7,c8,c10,c11,c17)
```

```

% Where
%=====
% Electrical Load Estimation
%=====
% a1=total load dc current requirments
% a2=average daily load usage
a3=a1*a2; % Average Daily Load
% a4=Nominal Load Voltage
% a5=maximum load DC Current
%=====
% Buttery Sizing
%=====
% b1=Autonomy Period
% b2=allowable max. depth of discharge
% b3=min. battery operating temp
% b4=battery capacity temp. derating factor
b5=(a3*b1)/(b2*b4);
% b6=nominal capacity of selected battery
% b7=Nominal Voltage of Selected Battery
b8=ceil(a4/b7); % No. of batteries in series
b9=ceil(b5/b6); % No. of batteries in parallel
b10=b8*b9; % Total No. Of Batteries
b11=b9*b6; % Total Battery Capacity
b12=(a3*100/b11); % Battery Daily Average of Discharge %
b13=b11/a5; % Battery Max. Discharge Rate (Functional -hours)
%=====
% PV Array Sizing
%=====
% c1=month;

```

```

% c2=design month insolation
% c3=Optimal Array Tilt Angle to Max. Insolation.
c4=a3;          % Average Daily Load Requirement
% c5=load adjustment factor for system inefficiencies (decimal)
c6=c4/c5;      % Adjusted Design Month Average Daily Load
% c7=selected module max. power current Imp
% c8=module output derating factor (decimal)
c9=c7*c8;      % Adjusted Module Max. Power Current Output
% c10=Selected Module Max. Power Voltage
% c11=Module Voltage Temp. Derating Factor (decimal)
c12=c10*c11;   % Temp. Derated Module Max. Power Voltage
c13=c2*c9;     % Module Daily Output
c14=ceil(c6/c13); % No. of Parallel Modules required
c15=ceil(a4/c12); % No. of Series Modules required
c16=c11*c12;
% c17=Nominal Rated PV Module Output
c18=c14*c13;   % Nominal Array Rated Output
%=====
% Sizing Summary
%=====
o1=a3;        % Lighting Load
o2=b1;        % Autonomy Period
o3=[b8 b9];   % Selected Batteries
o4=b11;       % BaTTERIES Selected Capacity
o5=100*b2;    % Allowable MDOD
o6=b12;       % Average MDDOD
o7=[c15 c14];
o8=c7*c14*c2/c4; % A:L Ratio

```

Appendix C

Abbreviations

a-Si	Amorphous Silicon
AC	Alternate Current
BIPV	Building Intergraded Photovoltaic
CdTe	Cadmium Telluride
CIS	Copper Indium diselenide
DC	Direct Current
DDOD	Daily Depth Of Discharge
DOD	Depth Of Discharge
EOD	End Of Discharge
EU	Europe Union
GEF	Global Environment Facility
HTT	Heterojunction with intrinsic thin layer
IEEE	Institute of Electrical and Electronics Engineer
I_{mp}	Current at Maximum Power Point
MDDOD	Maximum Daily Depth Of Discharge
MDOD	Maximum Depth Of Discharge
MPPT	Maximum Power Point Tracker
MSW	Municipal Solid Waste
OMSW	Oil Mill Solid Waste
PAPP	Programme of Assistance to the Palestinian People
PEC	Palestinian
PV	Photovoltaic
PWM	Pulse Width Modulation

SC	Solar Collector
SGP	Small Grants Program
UNDP	United Nation for Development Program
Vmpp	Voltage at Maximum Power Point
WTE	Wastes